33. Tate D, Paul RH, Flanigan TP, Tashima K, Nash J, Adair C, Boland R, Cohen RA (2003) The impact of apathy and depression on quality of life in patients infected with HIV. AIDS Patient Care STDS 17:115–120
34. Tombaugh TN (2004) Trail making test A and B: normative data stratified by age and education. Arch Clin Neuropsychol 19:203–214
35. Toronov V, Webb A, Choi JH, Wolf M, Michalos A, Gratton E, Hueber D (2001) Investigation of human brain hemodynamics by simultaneous near-infrared spectroscopy and functional magnetic resonance imaging. Med Phys 28:521–527
36. Wagner G, Sinsel E, Sobanski T, Kohler S, Marinou V, Mentzel HJ, Sauer H, Schlosser RG (2006) Cortical inefficiency in patients with unipolar depression: an event-related FMRI study with the Stroop task. Biol Psychiatry 59:958–965
37. Walter H, Berger M, Schnell K (2009) Neuropsychotherapy: conceptual, empirical and neuroethical issues. Eur Arch Psychiatry Clin Neurosci 259(Suppl 2):S173–S182
38. Walter H, Wolf RC, Spitzer M, Vasic N (2007) Increased left prefrontal activation in patients with unipolar depression: an event-related, parametric, performance-controlled FMRI study. J Affect Disord 101:175–185
39. Ware JE Jr, Sherbourne CD (1992) The mos 36-item short-form health survey (sf-36). I. Conceptual framework and item selection. Med Care 30:473–483
40. Zakzanis KK, Mraz R, Graham SJ (2005) An FMRI study of the trail making test. Neuropsychologia 43:1878–1886

OPEN ACCESS Freely available online PLoS one

The Effect of Negative and Positive Emotionality on Associative Memory: An fMRI Study

Go Okada[1,2]*, Yasumasa Okamoto[1,2], Yoshihiko Kunisato[1,3], Shiori Aoyama[1], Yoshiko Nishiyama[1], Shinpei Yoshimura[1], Keiichi Onoda[4], Shigeru Toki[1], Hidehisa Yamashita[1], Shigeto Yamawaki[1]

1 Department of Psychiatry and Neurosciences, Division of Frontier Medical Science, Programs for Biomedical Research, Graduate School of Biomedical Sciences, Hiroshima University, Hiroshima, Japan, **2** Core Research for Evolutional Science and Technology, Japan Science and Technology Corporation, Kawaguchi, Japan, **3** Research Fellow of the Japan Society for the Promotion of Science, Tokyo, Japan, **4** Department of Neurology, Shimane University, Izumo, Japan

Abstract

In general, emotion is known to enhance memory processes. However, the effect of emotion on associative memory and the underling neural mechanisms remains largely unexplored. In this study, we explored brain activation during an associative memory task that involved the encoding and retrieval of word and face pairs. The word and face pairs consisted of either negative or positive words with neutral faces. Significant hippocampal activation was observed during both encoding and retrieval, regardless of whether the word was negative or positive. Negative and positive emotionality differentially affected the hemodynamic responses to encoding and retrieval in the amygdala, with increased responses during encoding negative word and face pairs. Furthermore, activation of the amygdala during encoding of negative word and neutral face pairs was inversely correlated with subsequent memory retrieval. These findings suggest that activation of the amygdala induced by negative emotion during encoding may disrupt associative memory performance.

Citation: Okada G, Okamoto Y, Kunisato Y, Aoyama S, Nishiyama Y, et al. (2011) The Effect of Negative and Positive Emotionality on Associative Memory: An fMRI Study. PLoS ONE 6(9): e24862. doi:10.1371/journal.pone.0024862

Editor: Ben J. Harrison, The University of Melbourne, Australia

Received February 23, 2011; **Accepted** August 23, 2011; **Published** September 14, 2011

Funding: This research is supported by "creation of technology towards diagnosis and treatment besed on understanding of molecular pathogenesis of psychiatric and neurological disorders" the Core Research for Evolutional Science and Technology (CREST), Japan Science and Technology Corporation (JST). The funders had no role in study design, data collection and analysis, decision to publish, or preparation of the manuscript.

Competing Interests: The authors have declared that no competing interests exist.

* E-mail: goookada@hiroshima-u.ac.jp

Introduction

The ability to learn and remember new associations between previously unrelated information is an important aspect of declarative memory. Declarative memory is associative, linking together component parts, such as words and objects, either directly or via spatial, temporal or other relationships. Previous neuroimaging studies have provided crucial information concerning the neural correlates that underlie this process. A variety of associative encoding tasks results in robust hippocampal activation, including the encoding of word pairs [1,2,3,4] and triplets [5,6], object pairs [7], and name–face pairs [8,9,10].

On the other hand, the relationship between memory and emotion is of paramount importance, given that people experience various affective states over the course of daily life. Although a recent review on memory and emotion has demonstrated that emotion may enhance memory processes that occur at all stages, including encoding, storage, and retrieval [11], we previously reported that negative emotionality does not necessarily promote good memory performance and associated hippocampal activation [12]. This discrepancy may be due to procedural differences. The most likely explanation is that the encoding of an association between items may have played a key role. The possible effects of emotionality associated with memory for paired items is unclear, even though the medial temporal lobe (including the hippocampus) showed greater activation for emotional items than for neutral items during both encoding [13] and retrieval [14] in studies of memory for single items. Furthermore, although much functional neuroimaging evidence has linked the memory-enhancing effect of emotion to amygdalic modulation during encoding [13,15,16,17,18,19,20] and retrieval [14], whether similar emotionality effects can be observed on associative memory remains unclear. Indeed, emotion does not necessarily enhance memory. When faced with negative events, people tend to pay attention to central features of such events while ignoring peripheral details [21,22]. As a result, memory of the negative event itself is enhanced, whereas memory of peripheral events is impaired. Furthermore, the difference between memory for gist and memory for detail can be more pronounced for negative than for positive events [23].

In this study, we hypothesized that negative emotion does not necessarily promote good associative memory performance, and that the amygdala has disparate influences on associative memory for positive and negative information. We used fMRI to investigate the effect of emotional (negative or positive) item valence on brain activation during an associative memory task, and examined the relationship between memory performance and brain activation affected by emotion during encoding and retrieval.

Results

Behavioral results

During the fMRI protocol, 15 healthy volunteers performed a novel face-emotional word paired associate task consisted of 'encoding', in which subjects were asked to remember pairs of neutral face and emotional (positive or negative) words, and 'control' and 'retrieval', in which subjects were asked to indicate

the word that was previously paired with that face (Fig. 1; see Methods for details). The mean correct response rates (mean ± SD) during retrieval were 48.9±14.7% for negative word and neutral face pairs and 58.1±13.3% for positive word and neutral face pairs. Accuracy rates across the two emotional conditions differed significantly (paired t-test, $t=-2.208$, $p=0.044$).

Group analysis on each contrast

We performed fMRI group analysis on the four contrasts, subtracting the control condition from each experimental condition, according to a random effect model. All activations satisfying our criteria for significance are shown in Tables 1 and 2. We observed significant activation of the hippocampus during all of the 4 conditions, and significant activation of the left amygdala only during the negative encoding condition.

Correlation between activations in regions detected by one sample t-tests and associative memory performances

We conducted a secondary correlation analysis to examine the relationship between brain activation in regions detected by one sample t-tests and associative memory performance. There wasn't positive correlation between brain activation and associative memory performance in any areas. In contrast, this analysis revealed that left amygdala and hippocampus activation during encoding of negative word and neutral face pairs (contrast estimate of 'negative encoding – control') was inversely correlated ($r=-0.527$, $p=0.043$, and $r=-0.519$, $p=0.047$, respectively) with successful retrieval (Table 3).

Differential effects of negative and positive emotion on encoding and retrieval

A 2×2 ANOVA was performed to examine the differential effects of negative and positive emotion on encoding and retrieval. All activations satisfying our criteria for significance are shown in Table 4. This analysis revealed significant emotion×task interactions in the left amygdala (Fig. 2A). Post hoc analysis (corrected by Bonferroni) of the averages of contrast estimates of voxels in this cluster revealed that the 'Encoding of negative word and neutral face pairs' showed a greater BOLD response compared with the 'Encoding of positive word and neutral face pairs' ($F=7.761$, $p=0.012$) and the 'Retrieval of negative word and neutral face pairs' ($F=8.335$, $p=0.015$) in this area (Fig. 2B).

Correlation analysis between amygdala activation and associative memory performance

We conducted a secondary correlation analysis to examine the relationship between amygdala activation (mentioned above and shown in Fig. 2A) and the corresponding behavioral performance. This analysis revealed that amygdala activation during encoding of negative word and neutral face pairs (contrast estimate of 'negative encoding – control') was inversely correlated ($r=-0.850$, $p=0.00006$), and that during encoding of positive word and neutral face pairs (contrast estimate of positive encoding – control) was positively correlated ($r=0.599$, $p=0.018$) (Fig. 3A) with successful retrieval (Fig. 3B). Amygdala activation during retrieval was not significantly correlated with a correct response rate regardless of whether the words were positive ($r=0.274$, $p=0.322$) or negative ($r=-0.165$, $p=0.557$).

Discussion

In this study, we explored the effect of emotion on associative memory performance and its underling neural mechanisms. The hippocampus showed activations during the encoding and retrieval of word and face pairs regardless of whether the words were negative or positive. However, there wasn't positive correlation between activations in these regions and associative

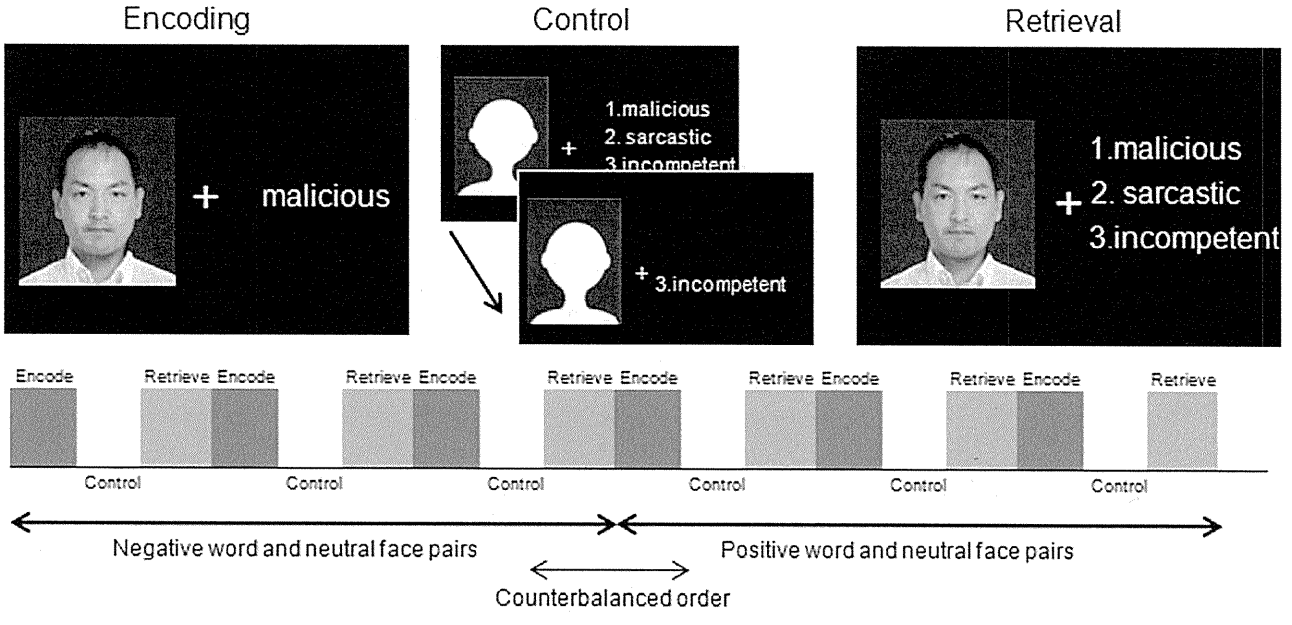

Figure 1. Face-Word Association Paradigm. Subjects were asked to learn pairs of neutral face and emotional (positive or negative) words related to personality-trait by pressing a button. After the control task in which subjects were asked to press one of the target button, each face was shown with 3 words and subjects were asked to indicate, via button press, which word was previously paired with that face. (The picture of one of the authors was used in the Figure instead of that from the database of SOFTPIA JAPAN to protect the privacy of subjects participated in the database).
doi:10.1371/journal.pone.0024862.g001

Table 1. Results of one sample t-test for negative word and neutral face pairs.

Region	BA	Side	peak level		cluster level		x	y	z
			Z	p	k_E	p			
Encoding									
Cerebellum		R	5.50	0.002	25	0.002	42	−52	−30
Inferior Frontal Gyrus	47	L	5.21	0.007	30	0.001	−42	−18	−10
Hippocampus		R	3.97	0.008[a]	71[a]	0.005[a]	28	−38	0
Hippocampus		L	3.37	0.050[a]	1[a]	0.044[a]	−30	−22	−16
Amygdala		L	2.91	0.050[b]	1[b]	0.046[b]	−30	0	−22
Retrieval									
Inferior Frontal Gyrus	47	L	5.70	0.001	132	0.000	−34	18	−6
Cerebellum		R	5.44	0.003	89	0.000	44	−54	−28
Precentral Gyrus	9	L	5.42	0.003	57	0.000	−38	4	38
Lingual Gyrus	18	L	5.34	0.004	451	0.000	−10	−82	−14
Cerebellum		L	5.29	0.005	92	0.000	0	−60	−44
Medial Frontal Gyrus	32	L	5.14	0.009	65	0.000	−8	12	50
Angular Gyrus	39	L	5.13	0.009	76	0.000	−32	−62	38
Cuneus	17	L	4.92	0.021	8	0.010	−24	−80	12
Middle Occipital Gyrus	19	L	4.83	0.030	19	0.003	−26	−92	4
Cerebellum		R	4.82	0.031	11	0.006	8	−74	−50
Superior Temporal Gyrus	38	L	4.76	0.036	4	0.018	−46	16	−16
Inferior Occipital Gyrus	18	L	4.74	0.042	5	0.015	−34	−88	−10
Cuneus	17	R	4.73	0.044	2	0.026	20	−96	−10
Hippocampus		L	3.65	0.023[a]	14[a]	0.023[a]	−24	−30	−6

BA, Brodmann area; L, Left; R, Right; Z, Z value of the peak activation within the cluster; Coordinates for the peak voxel are listed as MNI coordinates. p, corrected p value for whole brain or region of interest ([a] bilateral hippocampus which include 1667 voxels or [b] bilateral amygdala which include 306 voxels); k_E, cluster size (voxels) difined by the same peak-level FWE thresholds and used for the cluster level testing.

doi:10.1371/journal.pone.0024862.t001

Table 2. Results of one sample t-test for positive word and neutral face pairs.

Region	BA	Side	peak level		cluster level		x	y	z
			Z	p	k_E	p			
Encoding									
Cerebellum		R	4.85	0.031	5	0.013	42	−52	−30
Cerebellum		L	4.72	0.048	1	0.032	−6	−50	−40
Hippocampus		R	4.45	0.002[a]	103[a]	0.002[a]	36	−36	−6
Hippocampus		R	4.04	0.007[a]	4[a]	0.035[a]	40	−16	−22
Hippocampus		L	3.54	0.033[a]	13[a]	0.022[a]	−32	−22	−18
Hippocampus		L	3.49	0.038[a]	1[a]	0.043[a]	−26	−40	4
Retrieval									
Cerebellum		R	5.91	0.000	174	0.000	42	−54	−30
Middle Occipital Gyrus	18	L	5.89	0.000	877	0.000	−30	−34	−14
Insula	13	R	5.73	0.001	121	0.000	34	24	6
Precuneus	7	L	5.61	0.002	130	0.000	−28	−72	38
Medial Frontal Gyrus	6	L	5.46	0.003	234	0.000	−6	14	50
Inferior Frontal Gyrus	47	L	5.22	0.009	45	0.000	−34	18	−4
Inferior Occipital Gyrus	18	R	5.19	0.010	71	0.000	22	−92	−12
Cerebellum		R	5.10	0.014	8	0.006	10	−74	−34
Inferior Frontal Gyrus	9	L	5.05	0.017	128	0.000	−38	4	34
Fusiform Gyrus	19	R	4.98	0.023	13	0.002	32	−80	−20
Cerebellum		R	4.97	0.023	13	0.002	2	−62	−42
Cerebellum		R	4.94	0.026	11	0.003	36	−72	−28
Cuneus	18	L	4.88	0.033	5	0.010	−24	−82	12
Caudate		L	4.86	0.035	11	0.003	−12	−8	18
Inferior Frontal Gyrus		L	4.84	0.038	5	0.010	−46	16	2
Hippocampus		L	4.40	0.002[a]	114[a]	0.001[a]	−24	−30	−4
Hippocampus		R	4.12	0.006[a]	151[a]	0.000[a]	24	−26	−8

BA, Brodmann area; L, Left; R, Right; Z, Z value of the peak activation within the cluster; Coordinates for the peak voxel are listed as MNI coordinates. p, corrected p value for whole brain or region of interest ([a] bilateral hippocampus which include 1667 voxels or [b] bilateral amygdala which include 306 voxels); k_E, cluster size (voxels) difined by the same peak-level FWE thresholds and used for cluster level testing.

doi:10.1371/journal.pone.0024862.t002

memory performances, and on the contrary, there was significant negative correlations between left hippocampus activation during negative encoding and the rate of successful retrieval. In contrast, left amygdala activation was observed only during encoding with negative emotionality, and there was also significant negative correlations between this amygdala activation and successful retrieval. In addition, a 2×2 ANOVA and subsequent Post-hoc analysis detected the region activated specifically during encoding with negative emotionality in the left amygdala. Furthermore, this amygdala activation was inversely correlated with subsequent memory retrieval with high significance. These results suggest that amygdala activation induced by negative emotionality may disrupt associative memory encoding.

Although research on memory and emotion has demonstrated that emotional (both positive and negative) events are often better remembered than neutral events [13,14], we reported previously that negative emotionality does not enhance memory for associated word pairs [12]. In this study, we demonstrated that paired items with negative emotionality are more poorly remembered than those with positive emotionality. In this discrepancy, the encoding of an association between items may have played a role, as compared to encoding single items. This hypothesis is supported by the results of previous studies [21,22,24] demonstrating that negative emotion enhances memory for gist, but reduces memory for detail. Although the face and emotional word associative memory assessment in the present study are quite different from the gist and event detail assessments used by previous studies, it is possible that the negative word meanings operate as gist, while the relationships between word and face pairs operate as more peripheral, less salient aspect of the encoding task. This emotion-related effect of memory may be

Table 3. Correlation between activations in regions detected by one sample t-tests and associative memory performances.

	Region (peak coordinate)	Correct respons rate (negative)	Correct respons rate (positive)
Encoding (negative)	Hippocampus (28 −38 0)	$r=-0.446$, $p=0.096$	
	Hippocampus (−30 −22 −16)	$r=-0.527$, $p=0.043$*	
	Amygdala (−30 −0 −22)	$r=-0.519$, $p=0.047$*	
Retrieval (negative)	Hippocampus (−24 −30 −6)	$r=0.037$, $p=0.895$	
Encoding (positive)	Hippocampus (36 −36 −6)		$r=0.121$, $p=0.668$
	Hippocampus (40 −16 −22)		$r=0.130$, $p=0.643$
	Hippocampus (−32 −22 −18)		$r=-0.077$, $p=0.786$
	Hippocampus (−26 −40 4)		$r=-0.000$, $p=0.999$
Retrieval (positive)	Hippocampus (−24 −30 −4)		$r=-0.140$, $p=0.618$
	Hippocampus (24 −26 −8)		$r=0.079$, $p=0.780$

r, correlation coefficiency; *p*, p-value;
*, $p<0.05$.
doi:10.1371/journal.pone.0024862.t003

mediated by the amygdala, as suggested by the absence of the effect in individuals with amygdala damage [25]. However, the biological mechanism of such phenomenon has not been examined in detail in human functional neuroimaging studies. The pronounced inverse correlation between amygdala activation induced by negative emotionality and the correct response rate shown in this study provide direct evidence that amygdala activation during encoding is a mediator of this phenomenon.

Although we do not know the neural mechanisms responsible for the disruption of associative memory encoding with negative emotionality by amygdala activation, one possible mechanism is that amygdala activation enhances the attention to the negative word itself and reduces the attention to the association of the items required for task performance. This interpretation is consistent with the idea that the amygdala focuses processing resources on the most salient information, as Easterbrook originally proposed

Table 4. Results of 2×2 ANOVA.

Region	BA	Side	peak level		cluster level	x	y	z
			Z	p	k_E			
Main effect of task								
Encoding>Retrieval								
Angular Gyrus	39	L	6.46	0.000	312	−56	−62	38
Parahippocampal Gyrus	37	R	4.94	0.007	29	40	−38	−20
Superior Frontal Gyrus	9	L	4.71	0.020	7	−20	44	44
Superior Frontal Gyrus	6	L	4.56	0.038	2	−16	14	60
Middle Temporal Gyrus	39	L	4.53	0.042	2	−40	−66	16
Hippocampus		R	4.86	0.000[a]	112[a]	38	−18	−20
Hippocampus		L	3.56	0.024[a]	6[a]	−32	−26	−16
Retrieval>Encoding								
Inferior Occipital Gyrus	17	L	>8	0.000	13337	−10	−92	−12
Insula	13	R	5.72	0.000	217	32	26	2
Midbrain		L	5.63	0.000	500	−4	−20	−6
Inferior Frontal Gyrus	47	L	5.41	0.001	164	−30	22	−4
Inferior Frontal Gyrus	9	L	5.31	0.001	53	−58	4	30
Hippocampus		L	4.12	0.003[a]	8[a]	−20	−30	−4
Main effect of emotion								
No area								
Interaction Task×Emotion								
Amygdala		L	3.02	0.036[b]	6[b]	−24	−8	−16

BA, Brodmann area; L, Left; R, Right; Z, Z value of the peak activation within the cluster; Coordinates for the peak voxel are listed as MNI coordinates. p, corrected p value for whole brain or region of interest ([a] bilateral hippocampus which include 1667 voxels or [b] bilateral amygdala which include 306 voxels); k_E, cluster size (voxels) difined by the same peak-level FWE thresholds.
doi:10.1371/journal.pone.0024862.t004

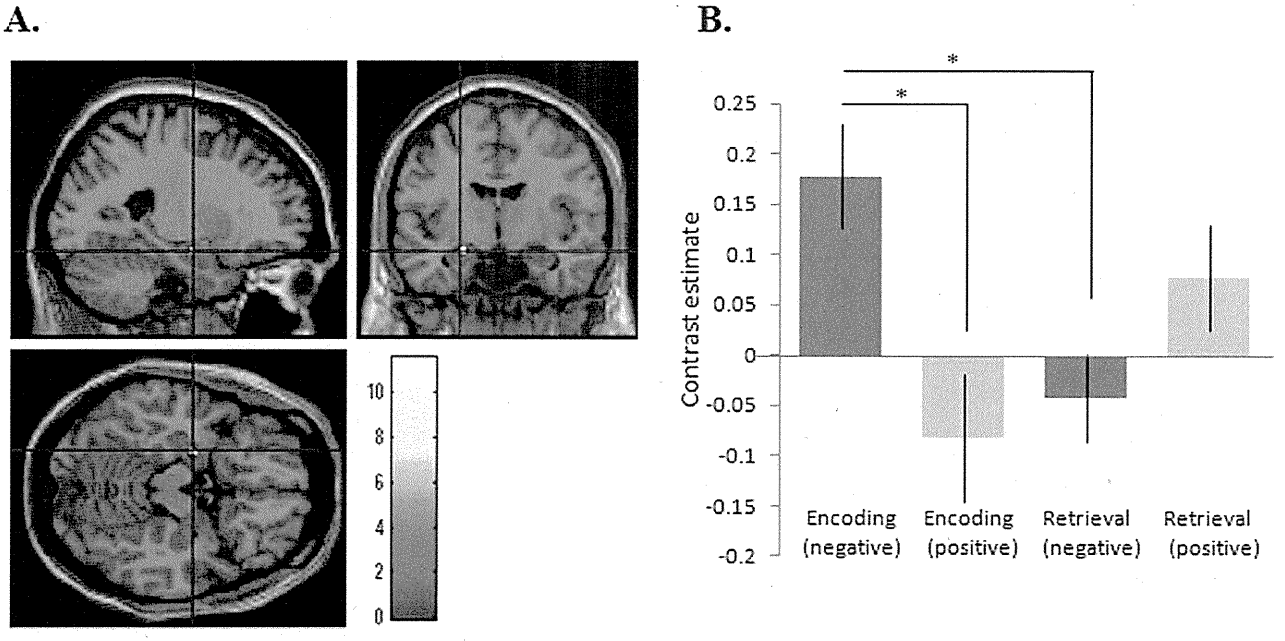

Figure 2. Differential effects of negative and positive emotion on encoding and retrieval. A. shows the brain region in which task×emotion interaction was detected (MNI coordinate: x = −24, y = −8, z = −16). B. shows the graph displaying the contrast estimates (mean ± SE) for the region of interest shown in Figure 2A for the 4 contrasts (negative encoding, positive encoding, negative retrieval, and positive retrieval compared to the relevant control) *: $p<0.05$.
doi:10.1371/journal.pone.0024862.g002

[26]. In fact, our regression analyses also revealed a significant inverse correlation between the correct response rate and the magnitude of brain activation in the left hippocampus. This means that activation of this region also disrupted rather than contributed to the associative memory processing. Given the fact that amygdala activity has been reported to correlate with subsequent memory for emotional material [15,16,27] and the influence of the amygdala on the efficacy of encoding is believed to be expressed through its effect on the hippocampus, it is plausible that the amygdala may focus processing recourses automatically on the negative words and not the association of paired items required for task performance.

In addition to the results mentioned above, amygdala activation during the positive encoding was positively correlated with the task performance of associative memory in this study. Although the mechanism of this inverse effect of amygdala activation on

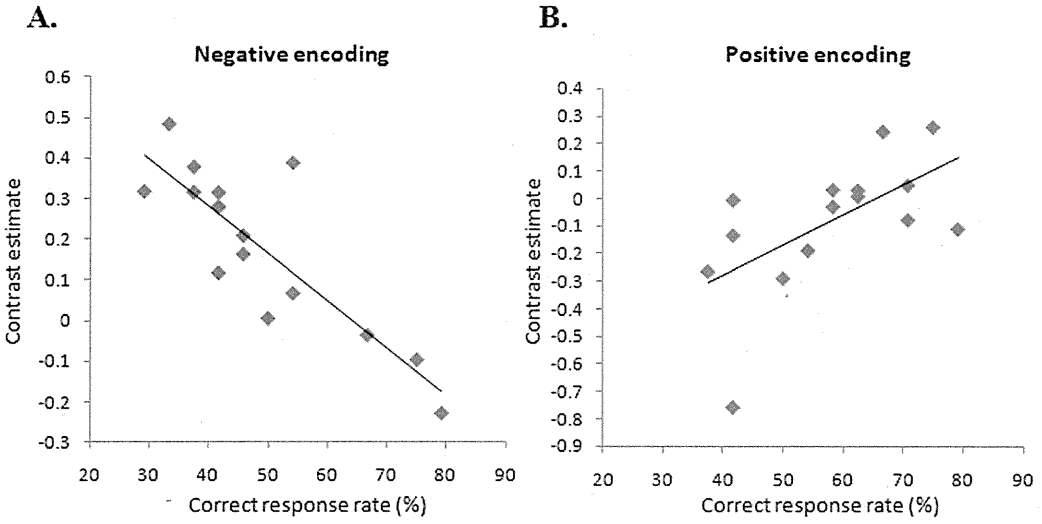

Figure 3. Correlation between amygdala activation and associative memory performance. A. shows the graph illustrates the inverse correlation between correct response rate of negative word - face pairs and the contrast estimates during encoding of negative word - face pairs in the region of interest shown in Figure 2A. B. shows the graph illustrates the positive correlation between correct response rate of positive word - face pairs and the contrast estimates during encoding of positive word - face pairs in the region of interest shown in Fig. 2A.
doi:10.1371/journal.pone.0024862.g003

associative memory is unclear, results of previous studies of patients with amygdalar damage suggest that the amygdala can both potentiate and reduce gist memory, depending on the encoding context [25]. Although additional research is required to better understand the circumstances (positive or negative, single item or paired item) in which amygdala activity can disrupt or facilitate memory encoding, the number of cues to which an organism attends may be modulated by emotional valence and not by arousal mediated by the amygdala.

There are certain limitations in this study that should be taken into consideration. First, we did not include a neutral word condition, so there is the possibility that the significant difference of associative memory performance between negative and positive condition was due to the enhancing effect of the positive word rather than the disrupting effect of the negative word. Although our previous study demonstrated that the correct response rate of negative word pairs was significantly lower than that of neutral word pairs [12], it remains unclear whether the effect of a negative word on face-word associative memory performance would be significant relative to neutral stimuli. However, it is plausible that amygdala activation during negative encoding disrupt the associative memory performance from the pronounced inverse correlation between amygdala activation and associative memory performance. Second, we did not evaluate unpleasantness during the task, so the direct relationship between amygdala activation and negative emotionality is not necessarily clear in this study, although it is reasonable to consider that amygdala activation was induced by negative emotionality of words. Third, as in previous studies [10,28], our control (baseline) task did not include real faces, so our results of one sample t-test included the regions which were related to the face perception as well as memory and emotion. However, face perception was equally included in each task (negative encoding, positive encoding, negative retrieval, or positive retrieval), and our results of a 2×2 ANOVA was never confounded by face perception. Fourth, we could not examine whether amygdala activation was positively or negatively correlated with the memory for the words themselves, so we could not directly compare the role of amygdala activation between single item memory and associative memory encoding. Further study is needed to address this issue. Finally, we did not use an event-related subsequent memory design which would be appropriate to directory justify the role of brain activation on associative memory performance, but the block-design in which we can raise the BOLD signal to measurable level in shorter scanning run. The major reason of this selection of design was that we were interested in examining the neural activity of associative memory performance in each individual subject, and applying such paradigm to psychiatric disorders like depression that cannot be forced into longer scanning run.

In conclusion, we observed that associative memory encoding is differentially modulated by amygdala activation according to the valence of emotionality. In particular, robust inverse correlation between the amygdala activation during encoding with negative emotionality and associative memory performance was observed. These findings suggest that amygdala activation induced by negative emotion may automatically focus processing resources on the most salient information, and disrupt associative memory encoding directed by instruction.

Materials and Methods

Ethics Statement

The study was conducted under a protocol that was approved by the Ethics Committee of Hiroshima University. All subjects submitted informed written consent of their participation.

Subjects

Fifteen healthy volunteers (6 men and 9 women), aged 21–27 years (mean age ± SD = 23.6±1.9 years), with no history of neurological or psychiatric illness, participated in the study. All subjects showed a similar level of intelligence as assessed by the Japanese Adult Reading Test (JART) (112.5±5.6).

Experimental task

During the fMRI protocol, subjects performed a novel block-designed face-emotional word paired associate task. We developed this task from a face-name paired associate task [10,28] that included 3 distinct conditions: encoding, distracter (active baseline), and recognition. The task consisted of 18 blocks, each of which was preceded by an instruction slide informing the subject whether the block was encoding, control, or retrieval condition. Of these 18 blocks, 6 were encoding conditions, 6 were control conditions, and 6 were retrieval conditions. Conditions were interleaved and repeated 6 times (Fig. 1). The duration of each condition was 24 seconds and the preceding instruction slide was shown for 4 seconds. This resulted in a total task period of 9 minutes.

During encoding, pairs of a face and an emotional word were presented serially every 3s, and subjects were asked to remember each face-emotional word pair by pressing a button. The active baseline (control) required subjects to press a button when 2 of 3 words disappeared (randomly within a 3s interval). We used the same emotional words during the corresponding control condition, so as to focus on how emotions modulate the associative memory processing and not on emotional responses themselves. During the retrieval condition, each face was shown with 3 emotional words every 3s, and the subjects were asked to indicate, via button press, which word was previously paired with that face. Forty-eight neutral faces paired with 6 emotional words (3 positive and 3 negative) were used during the experiment, because of the difficulty to select 48 appropriate emotional personality trait words. Although this means that the same words were repeatedly presented with different faces, a different face was presented every time and this task did not require the ability to overcome interference. That is, 48 pairs were presented within encoding condition, and no face-word pair was repeated during the experiment. Each retrieval block tested memory for only the pairs that were in the preceding encoding block, but the presentation of faces was not in the same order in the retrieval block as they were presented in the encoding block. Neutral faces were selected from the database of SOFTPIA JAPAN (The database is not available on line to protect the privacy of subjects participates in the database). Three positive words and 3 negative wards were selected from Anderson's list of personality-trait words translated into Japanese, and were rated on emotional valence and familiarity by a different group of participants [29]. Positive words were from the top 20 positive words and negative words were from the bottom 20 negative words of this list. Positive and negative words were matched in familiarity and word length. Each face and word pair was presented only once during the encoding tasks. For the retrieval tasks performed after the encoding tasks, the remaining 2 of the 3 words were used as distracters. The negative and positive conditions were counterbalanced across the subjects. Stimuli were generated using a personal computer with Presentation software (Neurobehavioral Systems, Inc.; San Francisco, CA). Using an angled mirror, participants viewed the stimuli on a back projection screen mounted outside the scanner bore.

Acquisition of MRI data

Imaging data were acquired using a GE 3.0 T scanner (General Electric, Milwaukee, Wisconsin). A time course series of 190

volumes per participant (including pre- and post-task period) was acquired with echo planar imaging sequences (TR = 3000 ms, TE = 27 ms, FA = 90deg, Matrix size = 64×64, FOV = 256 mm, 4 mm slice thickness, 32 slice, no gap). Functional scans lasted 9 minutes 30 seconds. After functional scanning, structural scans were acquired using T1-weighted gradient echo pulse sequences (TR = 7.2 ms, TE = 2.1 ms, FA = 20deg, Matrix size = 256×256, FOV = 256 mm, 1 mm slice thickness, 184 slice).

Analysis

Data were analyzed using the statistical parametric mapping software package, SPM8 (Wellcome Department of Cognitive Neurology, London, UK). The first 5 volumes of the fMRI run (pre-task period) were discarded to ensure a steady-state MR signal, and the remaining 185 volumes were used for the statistical analysis. Each set of functional volumes was realigned to the first volume, spatially normalized to a standard template based upon the Montreal Neurological Institute (MNI) reference brain, and spatially smoothed using an 8-mm FWHM Gaussian kernel.

We modeled four contrasts for each individual, using a general linear model that included each condition (negative encoding, positive encoding, negative retrieval, and positive retrieval) compared to the relevant control conditions. Then, second level analyses were performed according to a random effect model. First, one sample *t*-tests were performed for each contrast. The statistical threshold of $p<0.05$, corrected for whole-brain family wise error (FWE) at a peak level was used, except for *a priori* hypothesized regions, which were thresholded at $p<0.05$, and corrected for small volume (search volume is *a priori* region of interest mask) FWE at a peak level. These *a priori* regions of interest included the hippocampus and amygdala, a region implicated in the processing of memory and emotion. The hippocampal and amygdalic region of the interest mask was created in Montreal Neurological Institute (MNI) space using the WFU Pick Atlas [30]. We used WFU Pick Atlas only for creating the hippocampal and amygdalic region of interest mask, and all other analyses were conducted by using SPM 8.

Second, Pearson's correlation analyses were performed using the averages of contrast estimates (negative encoding-control, positive encoding-control, negative retrieval-control, and positive retrieval-control) of voxels within the clusters detected by the one sample t-test, in order to examine whether activations of these regions during each condition were correlated with corresponding memory performances. Third, a 2×2ANOVA with factors of task (encoding or retrieval) and emotion (negative or positive) was performed. The statistical threshold for this analysis was also set at $p<0.05$, corrected for FWE at a peak level, and small volume correction (SVC) were applied for the hippocampus and amygdala. Finally, Pearson's correlation analyses were performed using the averages of contrast estimates (negative encoding-control, positive encoding-control, negative retrieval-control, and positive retrieval-control) of voxels within the same amygdala cluster detected in the interaction task×emotion interaction shown in Fig. 2, in order to examine whether activations of this region during each condition was correlated with corresponding memory performances.

Acknowledgments

The authors would like to thank the MRI staff at the Hiroshima University Medical Hospital for use of facilities and technical support. Special thanks are due to Y. Akiyama for his contribution to the project. We also thank T. Matsumoto for helpful discussion.

Author Contributions

Conceived and designed the experiments: GO YO YK S. Yoshimura KO ST HY S. Yamawaki. Performed the experiments: GO YK SA YN. Analyzed the data: GO YK. Wrote the paper: GO YO YK KO S. Yoshimura S. Yamawaki.

References

1. Henke K, Weber B, Kneifel S, Wieser HG, Buck A (1999) Human hippocampus associates information in memory. Proc Natl Acad Sci U S A 96: 5884–5889.
2. Jackson O, 3rd, Schacter DL (2004) Encoding activity in anterior medial temporal lobe supports subsequent associative recognition. Neuroimage 21: 456–462.
3. Meltzer JA, Constable RT (2005) Activation of human hippocampal formation reflects success in both encoding and cued recall of paired associates. Neuroimage 24: 384–397.
4. Prince SE, Daselaar SM, Cabeza R (2005) Neural correlates of relational memory: successful encoding and retrieval of semantic and perceptual associations. J Neurosci 25: 1203–1210.
5. Lepage M, Habib R, Cormier H, Houle S, McIntosh AR (2000) Neural correlates of semantic associative encoding in episodic memory. Brain Res Cogn Brain Res 9: 271–280.
6. Addis DR, McAndrews MP (2006) Prefrontal and hippocampal contributions to the generation and binding of semantic associations during successful encoding. Neuroimage 33: 1194–1206.
7. Kohler S, Danckert S, Gati JS, Menon RS (2005) Novelty responses to relational and non-relational information in the hippocampus and the parahippocampal region: a comparison based on event-related fMRI. Hippocampus 15: 763–774.
8. Sperling RA, Bates JF, Cocchiarella AJ, Schacter DL, Rosen BR, et al. (2001) Encoding novel face-name associations: a functional MRI study. Hum Brain Mapp 14: 129–139.
9. Sperling R, Chua E, Cocchiarella A, Rand-Giovannetti E, Poldrack R, et al. (2003) Putting names to faces: successful encoding of associative memories activates the anterior hippocampal formation. Neuroimage 20: 1400–1410.
10. Zeineh MM, Engel SA, Thompson PM, Bookheimer SY (2003) Dynamics of the hippocampus during encoding and retrieval of face-name pairs. Science 299: 577–580.
11. LaBar KS, Cabeza R (2006) Cognitive neuroscience of emotional memory. Nat Rev Neurosci 7: 54–64.
12. Onoda K, Okamoto Y, Yamawaki S (2009) Neural correlates of associative memory: the effects of negative emotion. Neurosci Res 64: 50–55.
13. Dolcos F, LaBar KS, Cabeza R (2004) Interaction between the amygdala and the medial temporal lobe memory system predicts better memory for emotional events. Neuron 42: 855–863.
14. Dolcos F, LaBar KS, Cabeza R (2005) Remembering one year later: role of the amygdala and the medial temporal lobe memory system in retrieving emotional memories. Proc Natl Acad Sci U S A 102: 2626–2631.
15. Cahill L, Haier RJ, Fallon J, Alkire MT, Tang C, et al. (1996) Amygdala activity at encoding correlated with long-term, free recall of emotional information. Proc Natl Acad Sci U S A 93: 8016–8021.
16. Hamann SB, Ely TD, Grafton ST, Kilts CD (1999) Amygdala activity related to enhanced memory for pleasant and aversive stimuli. Nat Neurosci 2: 289–293.
17. Canli T, Desmond JE, Zhao Z, Gabrieli JD (2002) Sex differences in the neural basis of emotional memories. Proc Natl Acad Sci U S A 99: 10789–10794.
18. Kilpatrick L, Cahill L (2003) Amygdala modulation of parahippocampal and frontal regions during emotionally influenced memory storage. Neuroimage 20: 2091–2099.
19. Phelps EA (2004) Human emotion and memory: interactions of the amygdala and hippocampal complex. Curr Opin Neurobiol 14: 198–202.
20. Richardson MP, Strange BA, Dolan RJ (2004) Encoding of emotional memories depends on amygdala and hippocampus and their interactions. Nat Neurosci 7: 278–285.
21. Christianson SA (1992) Emotional stress and eyewitness memory: a critical review. Psychol Bull 112: 284–309.
22. Berntsen D (2002) Tunnel memories for autobiographical events: central details are remembered more frequently from shocking than from happy experiences. Mem Cognit 30: 1010–1020.
23. Denburg NL, Buchanan TW, Tranel D, Adolphs R (2003) Evidence for preserved emotional memory in normal older persons. Emotion 3: 239–253.
24. Adolphs R, Denburg NL, Tranel D (2001) The amygdala's role in long-term declarative memory for gist and detail. Behav Neurosci 115: 983–992.
25. Adolphs R, Tranel D, Buchanan TW (2005) Amygdala damage impairs emotional memory for gist but not details of complex stimuli. Nat Neurosci 8: 512–518.

26. Easterbrook JA (1959) The effect of emotion on cue utilization and the organization of behavior. Psychol Rev 66: 183–201.
27. Strange BA, Henson RN, Friston KJ, Dolan RJ (2000) Brain mechanisms for detecting perceptual, semantic, and emotional deviance. Neuroimage 12: 425–433.
28. Glahn DC, Robinson JL, Tordesillas-Gutierrez D, Monkul ES, Holmes MK, et al. (2010) Fronto-temporal dysregulation in asymptomatic bipolar I patients: A paired associate functional MRI study. Hum Brain Mapp.
29. Yoshimura S, Ueda K, Suzuki S, Onoda K, Okamoto Y, et al. (2009) Self-referential processing of negative stimuli within the ventral anterior cingulate gyrus and right amygdala. Brain Cogn 69: 218–225.
30. Maldjian JA, Laurienti PJ, Kraft RA, Burdette JH (2003) An automated method for neuroanatomic and cytoarchitectonic atlas-based interrogation of fMRI data sets. Neuroimage 19: 1233–1239.

Altered γ-secretase activity in mild cognitive impairment and Alzheimer's disease

Nobuto Kakuda[1,2,3], Mikio Shoji[4], Hiroyuki Arai[5], Katsutoshi Furukawa[5], Takeshi Ikeuchi[6], Kohei Akazawa[7], Mako Takami[2,3], Hiroyuki Hatsuta[8], Shigeo Murayama[8], Yasuhiro Hashimoto[9], Masakazu Miyajima[10], Hajime Arai[10], Yu Nagashima[11], Haruyasu Yamaguchi[12], Ryozo Kuwano[13], Kazuhiro Nagaike[1], Yasuo Ihara[2,14,3], the Japanese Alzheimer's Disease Neuroimaging Initiative*

Keywords: amyloid β-protein; CSF; γ-secretase; NSAID; stepwise processing

DOI 10.1002/emmm.201200214

Received December 21, 2010
Revised December 22, 2011
Accepted January 09, 2012

We investigated why the cerebrospinal fluid (CSF) concentrations of Aβ42 are lower in mild cognitive impairment (MCI) and Alzheimer's disease (AD) patients. Because Aβ38/42 and Aβ40/43 are distinct product/precursor pairs, these four species in the CSF together should faithfully reflect the status of brain γ-secretase activity, and were quantified by specific enzyme-linked immunosorbent assays in the CSF from controls and MCI/AD patients. Decreases in the levels of the precursors, Aβ42 and 43, in MCI/AD CSF tended to accompany increases in the levels of the products, Aβ38 and 40, respectively. The ratios Aβ40/43 *versus* Aβ38/42 in CSF (each representing cleavage efficiency of Aβ43 or Aβ42) were largely proportional to each other but generally higher in MCI/AD patients compared to control subjects. These data suggest that γ-secretase activity in MCI/AD patients is enhanced at the conversion of Aβ43 and 42 to Aβ40 and 38, respectively. Consequently, we measured the *in vitro* activity of raft-associated γ-secretase isolated from control as well as MCI/AD brains and found the same, significant alterations in the γ-secretase activity in MCI/AD brains.

INTRODUCTION

Senile plaques, the neuropathological hallmark of Alzheimer's disease (AD), are composed of amyloid β-protein (Aβ). Aβ is derived from β-amyloid precursor protein (APP) through sequential cleavage by β- and γ-secretases. β-Secretase cleaves at the luminal portion (β-site) of APP to generate a β-carboxyl terminal fragment of APP (βCTF), an immediate substrate of γ-secretase, to produce different Aβ species (for a review see Selkoe, 2001). The most abundant secreted Aβ species is Aβ40,

(1) Immuno-Biological Laboratories Co., Fujioka, Japan
(2) Faculty of Life and Medical Sciences, Department of Neuropathology, Doshisha University, Kyoto, Japan
(3) New Energy and Industrial Technology Development Organization (NEDO), Kanagawa, Japan
(4) Department of Neurology, Institute of Brain Science, Hirosaki University Graduate School of Medicine, Hirosaki, Japan
(5) Division of Brain Sciences, Department of Geriatrics and Gerontology, Institute of Development, Aging and Cancer, Tohoku University, Sendai, Japan
(6) Department of Neurology, Brain Research Institute, Niigata University, Niigata, Japan
(7) Department of Medical Informatics, Niigata University Medical and Dental Hospital, Niigata, Japan
(8) Department of Neuropathology, Tokyo Metropolitan Institute of Gerontology, Tokyo, Japan
(9) Department of Biochemistry, Fukushima Medical University, Fukushima, Japan
(10) Department of Neurosurgery, Juntendo University School of Medicine, Tokyo, Japan
(11) Department of Neurology, Graduate School of Medicine, University of Tokyo, Tokyo, Japan
(12) Gunma University School of Health Sciences, Maebashi, Japan
(13) Department of Molecular Genetics, Bioresource Science Branch, Center for Bioresources, Niigata University, Niigata, Japan
(14) Core Research for Evolutional Science and Technology (CREST), Japan Science and Technology Corporation, Tokyo, Japan
***Corresponding author:** Tel: +81 774 656058; Fax: +81 774 731922;
E-mail: yihara@mail.doshisha.ac.jp

whereas the species that has two extra residues (Aβ42) is a minor one (<10%); however, the latter is the one that deposits first and predominates in senile plaques (Iwatsubo et al, 1994).

Presenilin 1/2 make up the catalytic site of γ-secretase. The enzymatic properties of γ-secretase that cleave the transmembrane domain of βCTF have been an enigma, although recent studies provided partial elucidation of this mechanism (Qi-Takahara et al, 2005; Takami et al, 2009). γ-Secretase has two product lines, which successively convert the Aβ49 and Aβ48 that are generated by ε-cleavage, to shorter Aβs by releasing tri- or tetrapeptides in a stepwise fashion. Aβ49 is successively cleaved mostly into Aβ40 via Aβ46 and Aβ43, while Aβ48 is similarly cleaved into Aβ38 via Aβ45 and Aβ42 (see Fig 1). Importantly, the differences between the amounts of released tri- and tetrapeptides determine the levels of the different Aβ species produced (Takami et al, 2009). Thus, the true activity of γ-secretase is defined by the amounts of tri- and tetrapeptides released, but not by the amounts of Aβ species produced. Of note, the most abundant species Aβ40 is derived not from Aβ42, but from Aβ43. Also Aβ38 is derived mainly from Aβ42 (Fig 1). The longer Aβs in cerebrospinal fluid (CSF) including Aβ49 and 46 as well as Aβ48 and 45 must be generated at negligible levels, but may neither be secreted to the interstitial fluid (ISF) nor recruited to CSF. This suggests that the status of brain, and possibly neuronal, γ-secretase could be accurately assessed by measuring all four Aβ species generated by the two product lines of γ-secretase.

Using enzyme-linked immunosorbent assays (ELISAs), we quantified Aβ40 and 43 and Aβ38 and 42 in CSF samples from control subjects and mild cognitive impairment (MCI)/AD patients. The CSF concentrations of Aβ43 and Aβ42 were found to be significantly lower in MCI/AD compared with controls. The ratio of Aβ38/42, which represents the ratio of product/precursor and thus the cleavage efficiency of Aβ42, was plotted against the ratio of Aβ40/43, which represents the ratio of product/precursor in the other product line and thus the cleavage efficiency of Aβ43. The ratio of Aβ38/42 was largely proportional to that of Aβ40/43, indicating that the two cleavage processes are tightly coupled, but both were generally higher in MCI/AD patients compared to control subjects These results

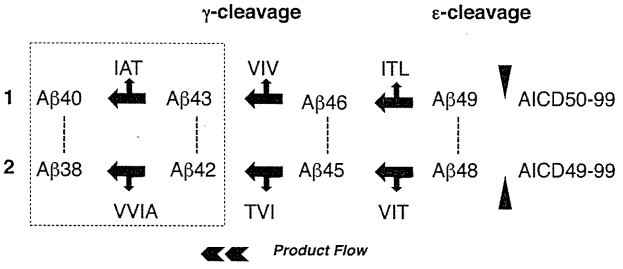

Figure 1. Generation of Aβs through stepwise processing of βCTF. At the first step, βCTF is cleaved at the membrane-cytoplasmic boundary (ε-cleavage), producing AICD (APP intracellular domain) 50–99 and 49–99. Counterparts Aβ49 and 48 in turn are cleaved in a stepwise fashion, releasing tri- and tetrapeptides. One product line converts Aβ49 mostly to Aβ40 via Aβ46 and Aβ43. The other product line converts Aβ48 to Aβ38 via Aβ45 and Aβ42. It should be noted that the differences between the amounts of released tri- or tetrapeptide determine the amounts of Aβs produced. Broken lines indicate corresponding Aβs on the two product lines.

suggest that the activity of brain γ-secretase in MCI/AD is enhanced at the conversion of Aβ43 to Aβ40 and Aβ42 to Aβ38, which would result in significantly lower CSF concentrations of Aβ42 and 43. In support of this hypothesis, the activities of raft-associated γ-secretase from control and MCI/AD brains were found to be significantly different: although the total Aβ production was similar, the γ-secretase in MCI/AD brains produced significantly larger ratios of Aβ40/43 and Aβ38/42 than the enzyme in control brains. This raises the possibility that lower CSF levels of Aβ42 and 43 simply reflect the altered γ-secretase activity in the MCI/AD-affected brains.

RESULTS

The CSF concentrations of Aβs were in the following order: Aβ40 > Aβ38 > Aβ42 ≫ Aβ43 in all CSF samples examined (Table 1 and Supporting Information Fig S2A). The relative amounts of Aβs were constant across the samples: Aβ38:40 ratio in CSF was ~1:3, and Aβ42:43 ratio was ~10:1. The CSF

Table 1. Subject characteristics and CSF concentrations of Aβs

	Control	MCI	AD	ANOVA ***p-value
Age (years)	74.9 ± 7.5	72.5 ± 6.6	72.3 ± 8.2	
N (male/female)	21 (10/11)	19 (7/12)	24 (7/17)	
MMSE score	28.7 ± 1.9	25.7 ± 2.6	19.6 ± 3.3	
ApoE ε4	3 (14.3%)	10 (52.6%) [a]	14 (58.6%) [a]	
Aβ38 (pM)	594.5 ± 286.3	669.4 ± 247.6	760.57 ± 269.4	
Ln(Aβ38)	6.28 ± 0.46	6.44 ± 0.38	6.56 ± 0.41	NS
Aβ40 (pM)	1607.9 ± 712.9	1939.5 ± 698.0	2292.6 ± 799.6	
Ln(Aβ40)	7.28 ± 0.47	7.51 ± 0.38	7.68 ± 0.35	0.007
Aβ42 (pM)	133.1 ± 53.4	83.2 ± 49.4**	90.3 ± 40.1 [a]	
Ln(Aβ42)	4.80 ± 0.47	4.25 ± 0.60	4.40 ± 0.47	0.004
Aβ43 (pM)	11.8 ± 5.7	6.8 ± 5.6**	7.0 ± 4.6**	
Ln(Aβ43)	2.32 ± 0.60	1.59 ± 0.86	1.76 ± 0.62	0.004

[a]2 MCI subjects were homozygous for ε4, while 4 AD subjects were homozygous for the allele.
**$p < 0.05$; Dunnett's *t*-test after log-transformation for comparing between control and MCI or AD.
***p-value of analysis of variance after log-transformation.

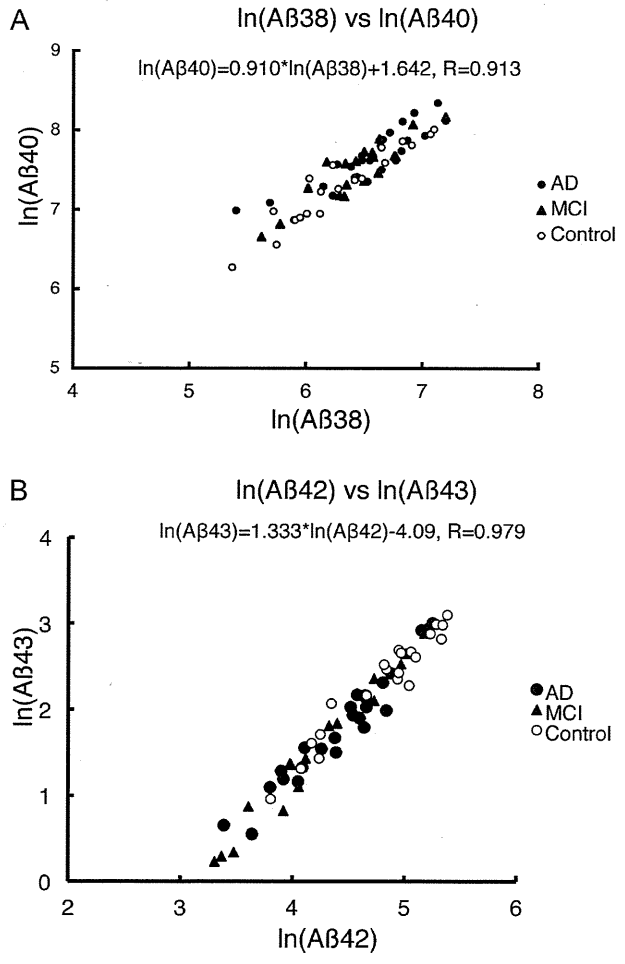

Figure 2. Relationships between the levels of Aβ40 and 38, and between those of Aβ43 and 42 in CSF from controls and MCI/AD patients.

A. The levels of ln(Aβ40) were proportional to those of ln(Aβ38) ($\ln(A\beta40) = 0.910 \times \ln(A\beta38) + 1.642$, $R = 0.913$).

B. The levels of ln(Aβ43) were proportional to those of ln(Aβ42) ($\ln(A\beta43) = 1.333 \times \ln(A\beta42) - 4.09$, $R = 0.979$). It should be noted that the levels of both ln(Aβ42) and ln(Aβ43) in MCI [filled triangle ($n = 19$)]/AD [filled circle ($n = 24$)] are lower than those in controls [open circles ($n = 21$)].

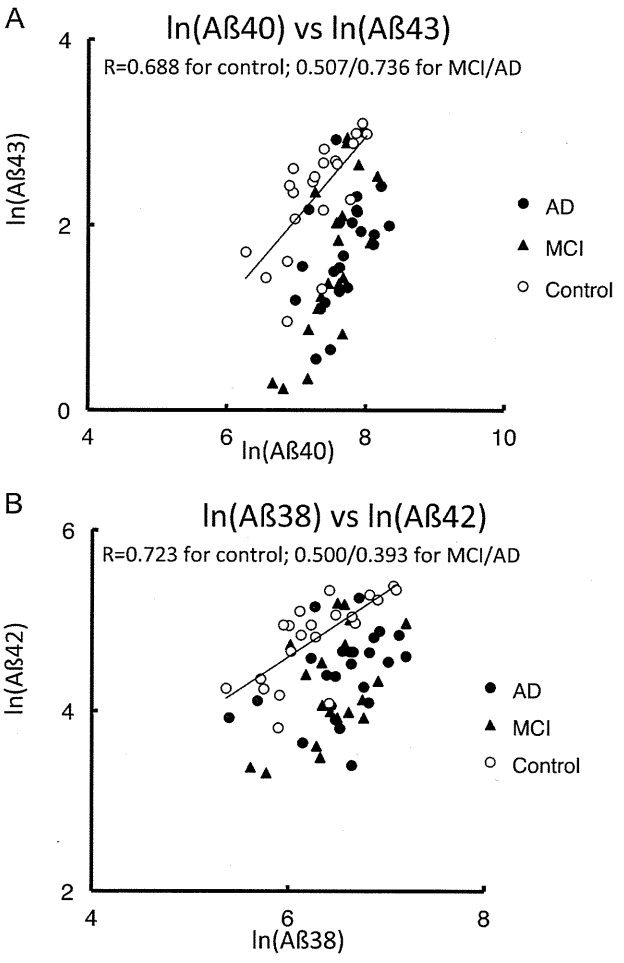

Figure 3. Relationships between the levels of Aβ43 and 40, and between those of Aβ42 and 38 in CSF from controls (open circles) and MCI (closed triangle)/AD patients (closed circle).

A. The levels of ln(Aβ43) correlate with those of ln(Aβ40) within controls ($R = 0.688$), and barely within MCI/AD subjects ($R = 0.507/0.736$). The plots for MCI/AD were located below the regression line for control ($p < 0.001$, ANOVA).

B. The levels of Aβ42 correlate with those of Aβ38 within controls ($R = 0.723$), and barely within MCI/AD ($R = 0.500/0.393$). The plots for MCI/AD were situated below the regression line for controls ($p < 0.001$, ANOVA).

concentrations of Aβ40 were significantly increased in AD compared to control (Table 1; $p < 0.05$, Dunnett's t-test). Additionally, the CSF concentrations of Aβ38 tended to be increased in AD patients compared to controls. In contrast, those of Aβ42 and 43 were significantly decreased in MCI/AD compared to controls ($p < 0.05$, Dunnett's t-test). Interestingly, as reported previously (Schoonenboom et al, 2005), the CSF concentrations of Aβ40 and Aβ38 were proportional to each other in all subjects [Fig 2A; $\ln(A\beta40) = 0.910 \times \ln(A\beta38) + 1.642$, $R = 0.913$, where ln(Aβ40) is the logarithm of Aβ40], even in MCI/AD cases. This was despite the fact that these species are derived from and the final products of the two different product lines of γ-secretase activity (Fig 1; Takami et al, 2009). In other words, the amounts of products in the third step of cleavage were strictly proportional to each other across the product lines.

Aβ42 and Aβ43 are produced by the second cleavage step of each product line. Like Aβ40 and Aβ38, the CSF concentrations of Aβ42 and Aβ43 are also proportional to each other in controls and in MCI/AD patients [Fig 2B; $\ln(A\beta43) = 1.333 \times \ln(A\beta42) - 4.09$, $R = 0.979$]. On the other hand, the levels of Aβ43 and Aβ40 (a precursor and its product) were correlated in control [Fig 3A; $\ln(A\beta43) = 0.884 \times \ln(A\beta40) - 4.118$, $R = 0.688$] and in MCI/AD subjects ($R = 0.507/0.736$ for MCI/AD, respectively) but the MCI/AD values were located below the regression line for controls and thus provided lower Aβ43 measures compared with controls for a given Aβ40 measure (Fig 3A; $p < 0.001$, analysis of variance, ANOVA). Conversely,

for a given Aβ43 value, the plot provided a higher Aβ40 measure in MCI/AD cases. There was a similar situation for the levels of Aβ42 and Aβ38. The levels of Aβ42 and Aβ38 were correlated each other in control subjects [Fig 3B; $\ln(A\beta42) = 0.724 \times \ln(A\beta38) + 0.251$, $R = 0.723$], but barely in MCI/AD ($R = 0.500$ for MCI; 0.393 for AD), and the MCI/AD plots were situated below the regression line for controls ($p < 0.001$, ANOVA). For a given Aβ42 value, the plot provided a higher Aβ38 measure in MCI/AD compared with controls.

These lower concentrations of Aβ42 appeared to be compensated with higher concentrations of Aβ38 as the levels of $\ln(A\beta38 + A\beta42)$ did not vary even in MCI/AD ($p = 0.293$, ANOVA). Thus, this points to the possibility that more Aβ42 and Aβ43 are converted to Aβ38 and Aβ40, respectively, in MCI/AD brains. According to numerical simulation based on the stepwise processing model, as the levels of βCTF decline to null, the levels of Aβ43 and 42 decrease and the ratios of Aβ40/43 and Aβ38/42 increase (unpublished observation). However, this situation can be excluded as the mechanism for lower concentrations of Aβ42 and 43, because the levels of βCTF have never been reported to be reduced in AD brains nor in plaque-forming Tg2576 mice that show lower CSF Aβ42 concentrations (Kawarabayashi et al, 2001). Thus, it is reasonable to suspect that the final cleavage steps from Aβ43 mostly to 40 and from Aβ42 to 38 are significantly enhanced in parallel (increases in released tri- and tetrapeptides) in brains affected by MCI/AD compared with controls (Fig 1).

This relationship in γ-secretase cleavage becomes clearer by plotting the product/precursor ratio representing cleavage efficiency at the step from Aβ42 to 38 (Aβ38/42) against that representing the cleavage efficiency at the step from Aβ43 to 40 (Aβ40/43) (Fig 4). The 'apparent' cleavage efficiency of Aβ43 was approximately 40-fold larger than that of Aβ42. The two ratios in CSF samples from MCI/AD and control subjects were largely proportional to each other, indicating that the corresponding cleavage processes in the two lines are tightly coupled (Fig 4). All plots were situated on a distinct line [$\ln(A\beta38/42) = 0.748 \times \ln(A\beta40/43) - 2.244$, $R = 0.936$] and its close surroundings. An increase in the cleavage from Aβ43 to 40 (*i.e.* more Aβ43 is converted to Aβ40) accompanied an increase in the cleavage from Aβ42 to 38 and *vice versa*, although the mechanism underlying this coupling between the two product lines remains unknown. This reminds us of the 'NSAID effect' in the 3-([3-cholamidopropyl]dimetylammonio)-2-hydroxy-1-propanesulfonate (CHAPSO)-reconstituted γ-secretase system (Takami et al, 2009; Weggen et al, 2001) in which the addition of sulindac sulfide to the γ-secretase reaction mixture, as expected, significantly suppressed Aβ42 production and increased Aβ38 production presumably by increasing the amounts of released tetrapeptide (VVIA) (Takami et al, 2009) and other peptides.

Most importantly, this graph provides a clear distinction between the control and MCI/AD groups (Fig 4; Aβ40/43 for MCI/AD *vs.* control, $p = 0.000$; Aβ38/42 for MCI/AD *vs.* control, $p = 0.000$; ANOVA, followed by Dunnett's *t*-test). The control values plotted close to the origin, whereas those for MCI/AD patients were distant from the origin along the line [$\ln(A\beta38/42) = 0.748 \times \ln(A\beta40/43) - 2.244$, $R = 0.936$]. It is also of note

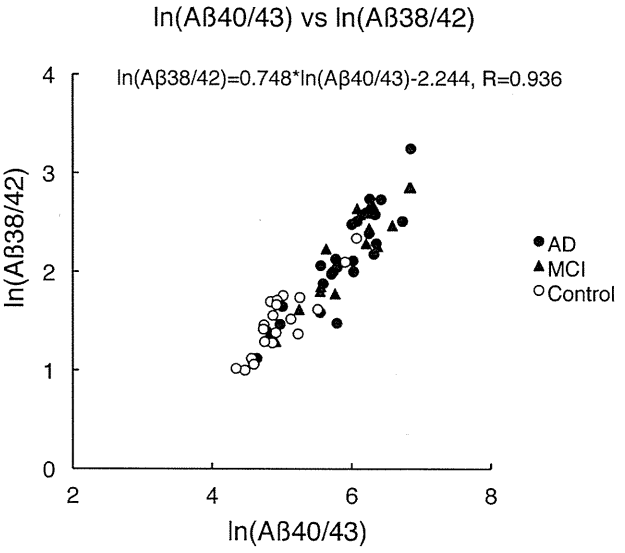

Figure 4. Ln(Aβ40/43) *versus* ln(Aβ38/42) plot. The ratios represent the cleavage efficiency at the final step of each line. Both ratios are largely proportional to each other ($y = 0.748 \times -2.244$, $R = 0.936$) and plots are located on the line and its close surroundings. This plot clearly distinguishes between control subjects and MCI/AD patients (Aβ40/43 for MCI *vs.* control, $p = 0.000$; Aβ38/42 for MCI *vs.* control, $p = 0.000$; ANOVA, followed by Dunnett's *t*-test). Control plots [open circles ($n = 21$)] are located close to the origin and MCI/AD plots [closed triangles ($n = 19$) and closed circles ($n = 24$), respectively] are a little distant from the origin.

that there was no significant difference between MCI and AD patients (Fig 4; Aβ40/43 for AD *vs.* MCI, $p = 1.000$; Aβ38/42 for AD *vs.* MCI, $p = 1.000$; Bonferroni's *t*-test). Two control values were a little farther from the origin, which may suggest that these subjects already have latent Aβ deposition or are in the preclinical AD stage. Additionally, we examined quite a small number of CSF samples from presenilin (PS) 1-mutated (symptomatic) familial AD (FAD) patients (T116N, L173F, G209R, L286V and L381V). Out of the three FAD cases near the regression line, two (T116N and L286V) were distant from the origin like sporadic AD cases and one (L381V) was closer to the origin than controls (both Aβ42/43 levels were lower than control; unpublished data). The remaining two (G209R and L173F) were extremely displaced from the line. Thus, a larger number of FAD cases are needed to give an appropriate explanation for their unusual characteristics in the plot, and the alteration of CSF Aβs shown above seems to be applicable only for sporadic AD.

Altogether, in MCI/AD, more Aβ42 and 43 are processed to Aβ38 and 40, respectively, than in controls. Even in MCI/AD, strict relationships are maintained between the levels of Aβ42 and Aβ43, and between those of Aβ38 and Aβ40 as seen in controls, which are predicted by the stepwise processing kinetics (unpublished observation). Thus, our observations suggest that lower CSF concentrations of Aβ42 and 43 and presumably higher CSF concentrations of Aβ38 and 40 are the consequence of altered γ-secretase activity in brain rather than the effect of preferential deposition of the two longer Aβ species (Aβ42 and 43) in senile plaques, which would not have maintained such strict relationships between the four Aβ species in CSF.

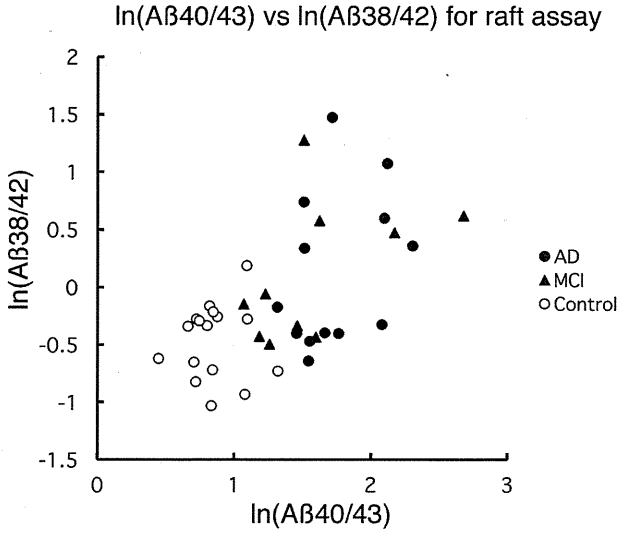

Figure 5. Ln(Aβ40/43) *versus* ln(Aβ38/42) plot based on direct quantification of raft-associated γ-secretase activity. The raft-associated γ-secretase prepared from control and MCI/AD brain specimens was incubated with βCTF for 2 h at 37°C (see Materials and Methods Section). Produced Aβs were quantified by Western blotting using specific antibodies. This plot distinguishes between control subjects and MCI/AD patients (Aβ40/43 for control *vs.* MCI/AD, $p < 0.001$; Aβ38/42 for control *vs.* MCI/AD, $p = 0.001$; Welch's *t*-test). MCI/AD plots [closed triangles ($n = 10$) and closed circles ($n = 13$), respectively] are as a whole a little distant from the origin, whereas control plots [open circles ($n = 16$)] are close to the origin.

To further test our hypothesis, we directly measured γ-secretase activities associated with lipid rafts isolated from AD, MCI and control cortices (Brodmann areas 9–11). For definite confirmation of the Aβ species, the reaction mixtures were subjected to quantitative Western blotting using specific antibodies rather than ELISA. At time 0, deposited Aβ42/43 species were detected in rafts from MCI/AD brains but not in control specimen (Supporting Information Fig S3). The amounts of ln(Aβ38 + Aβ42), which reflect the total capacity of the Aβ38/42-producing line, did not vary between AD, MCI and controls (Supporting Information Fig S4; $p = 0.969$, ANOVA). Thus, the gross activities of raft γ-secretase were comparable among the three groups. However, the plotted values for Aβ40/43 *versus* Aβ38/42 are divided into two groups: MCI/AD and controls (Fig 5; Aβ40/43 for control *vs.* MCI/AD, $p < 0.001$; Aβ38/42 for control *vs.* MCI/AD, $p = 0.001$; Welch's *t*-test) in the same way as those derived from CSF (Fig 4). It is notable that Figs. 4 and 5 are based on different methods, ELISA and Western blotting, respectively, but give similar results. There were no significant differences between MCI and AD specimen, although MCI patients (91 ± 4.9-year-old) were older than controls (77 ± 6.5-year-old) or AD patients (80 ± 5.0-year-old) (Aβ40/43 for MCI *vs.* AD, $p = 0.342$; Aβ38/42 for MCI *vs.* AD, $p = 0.911$). There were similar significant differences between control *versus* AD in the groups of which the ages were not significantly different (Aβ40/43 for control *vs.* AD, $p < 0.001$; Aβ38/42 for control *vs.* AD, $p = 0.03$).

DISCUSSION

Here, we assume that (i) Aβs in CSF are produced exclusively by γ-secretase in the brain, possibly in neurons; and (ii) Aβs in CSF are in the steady state. With these assumptions, the combined measurement of four Aβ species in CSF should predict the activity of γ-secretase in the brain. Here, the alterations in the γ-secretase activities do not mean the gross activity, *i.e.* total Aβ production, but the cleavage efficiency of the intermediates, Aβ42 and Aβ43.

In the present study, we quantified in CSF the four Aβ species, Aβ38/42 and Aβ40/43, but the Western blotting indicated the presence of additional Aβ species, Aβ37 and 39, in CSF (Supporting Information Fig S2). At present, we cannot exclude the possibility that a certain carboxyl terminus-specific protease(s) in CSF acts on the pre-existing Aβ species and converts them to Aβ37 and 39 (Zou et al, 2007). However, according to our unpublished data (Takami et al, unpublished observations), it is plausible that Aβ37 is derived from Aβ40, whereas Aβ39 is derived from Aβ42. Even if so, these pathways are very minor (~20–100-fold less) compared to the two major pathways, Aβ42 to Aβ38, and Aβ43 to Aβ40, when assessed by a reconstituted system (Takami et al, 2009). Thus, such strict relationships between four Aβs may have been relatively independent of Aβ37 and 39. The detailed relationship between all Aβs in the CSF awaits further quantification of the additional two Aβ species.

Currently, we do not know why the observation that Aβ40 is higher in MCI/AD CSF has so far not been reported except a recent paper (Simonsen et al, 2007). In fact, some of us previously reported no significant differences in CSF Aβ40 between AD and control subjects using a different ELISA (Shoji et al, 1998). It may be notable that we used newly constructed ELISA for Aβ40 based on a different set of monoclonal antibodies and thus, those discrepancies may come from the different antibody/epitope combination used for ELISA and/or different assay methods. In particular, it should be noted that all ELISAs used here detect Aβ1-x only, but not amino-terminally truncated forms. In this context, the ratio of Aβ40/43 appears to be more informative to discriminate between control and MCI/AD than the absolute levels of Aβ40 alone (Table 1 and Fig 5). It is possible that even if Aβ40 is not different between control and MCI/AD, the ratio Aβ40/43 could discriminate them.

We are the first to measure CSF Aβ43 using ELISA. The CSF concentrations of Aβ43 are 10-fold less than those of Aβ42. Nevertheless, the specificity of the newly constructed ELISA made the quantification of accurate levels of Aβ43 possible (Supporting Information Fig S1). Regarding the Aβ43 measures, we observed that its behaviour is entirely similar to that of Aβ42 in MCI/AD. Our preliminary observations using immunocytochemistry and ELISA quantification strongly suggest that Aβ43 deposits in aged human brains at the same time as Aβ42 (unpublished observations). Furthermore, Saido and colleagues have only recently reported that a PS1 R278I mutation in mice (heterozygous) caused an elevation of Aβ43 and its early and pronounced accumulation in the brain (Saito et al, 2011). It is possible that the cleavage of βCTF by this R278I γ-secretase may

be profoundly suppressed in the third cleavage step of the product line 1 (see Fig 1), which would result in negligible levels of Aβ40 and unusually high levels of Aβ43 (Nakaya et al, 2005). These results suggest that the role of Aβ43 should be reconsidered for the initiation of β-amyloid deposition and thus in AD pathogenesis.

Lower CSF concentrations of Aβ42 and 43 are not exclusively limited to MCI/AD. For example, similar low concentrations of Aβ42 and 43 were found in the CSF from eight patients with idiopathic normal pressure hydrocephalus (iNPH) (Aβ42, 76.3 ± 37.3 pM, $p = 0.012$ compared to controls: Aβ43, 5.2 ± 2.9 pM, $n = 8$, $p = 0.004$ compared to controls: Bonferroni's *t*-test; Silverberg et al, 2003). Thus, lower CSF concentrations of Aβ42 and 43 alone were unable to distinguish between iNPH and MCI/AD, and further, it is claimed that the former is often associated with abundant senile plaques, raising the possibility that Aβ deposition is enhanced by iNPH (Silverberg et al, 2003). However, when their partners Aβ38 and 40 were measured in CSF, both were found not to be significantly increased in iNPH (Aβ38, 459.2 ± 138.5 pM, $p = 0.484$ compared to controls; Aβ40, 1094.4 ± 375.3 pM, $n = 8$, $p = 0.103$ compared to controls; Table 1) in sharp contrast to MCI/AD indicating that the cleavage in iNPH at the steps from Aβ43 to 40 and from Aβ42 to 38 is not enhanced as it is in MCI/AD. Thus, it may be that the dilution effect elicited by ventricular enlargement would be the cause of lower CSF Aβ42 and 43 found in iNPH.

Currently, we do not know the mechanism behind the altered activity of brain γ-secretase in MCI/AD (Fig 4). First, it is of note that rafts prepared from MCI/AD brains but never from control brains at SP stage 0/A accumulated Aβ42 and Aβ43 (Supporting Information Fig S3; Oshima et al, 2001). It is possible that raft-deposited Aβ42/43 could induce a change in the γ-secretase activity, although the extent of the alteration in the activity appears not to be related to the extent of accumulation (unpublished observation). In this regard, it is of interest to note that Tg2576 mice, the best characterized AD animal model, shows reduced levels of Aβ42 in plasma as well as in CSF at the initial stage of Aβ deposition (Kawarabayashi et al, 2001). If the assumption here is correct, this may suggest that γ-secretase that produces plasma Aβs could also be altered. However, thus far, we have failed to replicate significantly lower Aβ42 levels or Aβ42/Aβ40 ratios in plasma from AD patients.

Second, there could be heterogenous populations of γ-secretase complexes that have distinct activities due to subtle differences in their components. γ-Secretase is a complex of four membrane proteins including PS, nicastrin (NCT), anterior pharynx defective 1 (Aph1) and presenilin enhancer 2 (Pen 2) (Takasugi et al, 2003). Aph 1 has three isoforms, and each can assemble active γ-secretase together with other components (Serneels et al, 2009). NCT, a glycoprotein, is present in immature and mature forms (Yang et al, 2002). The abundance of these heterogenous populations of proteins in the brain is probably under strict control. During MCI/AD, a certain population could replace other populations of γ-secretase and thus may show a distinct activity as a whole.

The data shown here represent only a cross-sectional study, but our keen interest is how the CSF levels of the four Aβ species would shift during the longitudinal course in an individual who is going to develop sporadic AD. Does one have any period during life when Aβ42 and 43 are at higher levels in CSF, and thus the ratios of Aβ38/42 and Aβ40/43 are smaller? At this period when the final cleavage steps of γ-secretase would be suppressed, the ISF concentrations of Aβ43 and 42 would increase, which would start or promote their aggregation in the brain parenchyma. If so, during life span, the individual's plot would move down along the regression line and move up as senile plaques accumulate, and the individual would eventually develop sporadic AD. However, thus far the period when there are increases in CSF Aβ42/43 has never been reported for sporadic AD. Nor has it been reported for asymptomatic FAD carriers (Ringman et al, 2008), whereas their plasma is known to contain higher levels (and percent) of Aβ42 (Kosaka et al, 1997; Ringman et al, 2008; Scheuner et al, 1996). It is likely that the stage of normal cognition and Aβ accumulation already accompanies reduced CSF Aβ42. If so, the alterations of γ-secretase should continue on for decades. Most interestingly, this alteration of CSF Aβ regulation seems to be planned to prevent further accumulation of Aβ42 and 43 in the brain.

However, Hong et al (2011) have recently shown, using *in vivo* microdialysis to measure ISF Aβ in APP transgenic mice, that the increasing parenchymal Aβ is closely correlated with decreasing ISF Aβ, suggesting that produced Aβ42 is preferentially incorporated into existing plaque-Aβ. This is a prevailing way of the interpretation of the data. Another way of the interpretation of data would be that during aging from 3 to 24 months, γ-secretase activity becomes altered and produces decreasing amounts of Aβ but with an increasing ratio of Aβ38/42 (and Aβ40/43). It is worth to mention that produced Aβ42 (but not Aβ40) appears to be selectively bound to rafts (from CHO cells) after long incubation (>4 h; Wada et al, unpublished observation). Also of note is that we quantified the total (free and bound) Aβ produced by an *in vitro* reconstituted system (Fig 5). What is claimed here is that decreased levels of CSF Aβ42 are largely due to alterations of γ-secretase activity rather than due to selective deposition of Aβ42 in preexisting plaques. What proportions of decreased ISF (CSF) Aβ42 levels would be contributed to by altered γ-secretase activity and selective deposition of Aβ42/43 to parenchymal plaques awaits future studies.

Finally, our observation has therapeutic implication. As shown elsewhere and here above, if Aβ42 is the culprit for MCI/AD, non-steroidal anti-inflammatory drugs (NSAIDs) would have been quite a reasonable therapeutic compound, which enhances cleavage at the third step in the stepwise processing, leading to lower levels of Aβ42 without greatly interfering with the Aβ bulk flow (Weggen et al, 2001). This sharply contrasts with some of the γ-secretase inhibitors currently under development and in clinical trial, which block the Aβ bulk flow. However, the present study raises the possibility that even if NSAIDs are administered, the expected beneficial effect could be minimal in MCI/AD patients, because in these patient brains, γ-secretase is already shifted to an NSAID-like effect.

MATERIALS AND METHODS

Subjects

Cerebrospinal fluid samples from 24 AD patients (mild to moderate AD; 50–86 years old), 19 MCI patients (57–82 years old) and 21 control subjects (61–89 years old) were collected (see Table 1) at Department of Neurology, Hirosaki University Hospital and at Department of Geriatrics and Gerontology, Tohoku University Hospital, and at Department of Neurology, Niigata University Hospital. The CSF samples from (symptomatic) 5 FAD (mPS1) patients (T116N, L173F, G209R, L286V and L381V) were from Niigata University Hospital. Probable AD cases met the criteria of the National Institute of Neurological and Communicative Disorders and Stroke–Alzheimer's Disease and Related Disorders (NINCDS-ADRDA) (Kuwano et al, 2006; McKhann et al, 1984). Additional diagnostic procedures included magnetic resonance imaging. Dementia severity was evaluated by the Mini-Mental State Examination (MMSE). Diagnosis of MCI was made according to the published criteria (Winblad et al, 2004). Diagnosis of iNPH was made according to the guideline issued by the Japanese Society of NPH (Ishikawa et al, 2008). Controls who had no sign of dementia and lived in an unassisted manner in the local community were recruited. All individuals included in this study were Japanese and 24 AD patients examined here were judged to have sporadic AD because of negative family history. This study was approved by the ethics committee at each hospital or institute.

Human cortical specimens for quantification of raft-associated γ-secretase activity were obtained from those brains that were removed, processed and placed in −80°C within 12 h postmortem [Patients were placed in a cold (4°C) room within 2 h after death] at the Brain Bank at Tokyo Metropolitan Institute of Gerontology. For all the brains registered at the bank we obtained written informed consents for their use for medical research from patient or patient's family. Each brain specimen (~0.5 g) were taken from Brodmann areas 9–11 of 13 AD patients [80 ± 5.0 years of age, Braak NFT stage > IV, SP stage = C (retrospective) CDR ≫ 1], 10 MCI patients (91 ± 4.9 years of age, Braak NFT stage < IV, SP stage < C, CDR = 0.5) and 16 controls (77 ± 6.5 years of age, Braak NFT stage < I, SP stage = 0/A, CDR = 0) (Adachi et al, 2010; Li et al, 1997).

Cerebrospinal fluid analysis

Cerebrospinal fluid (10–15 ml) was collected in a polypropylene or polystyrene tube and gently inverted. After brief centrifugation CSF was aliquotized to polypropylene tubes (0.25–0.5 ml), which were kept at −80°C until use. In our experience, Aβ42 (possibly, other Aβ species too) are readily absorbed even to polypropylene tubes (~20% per new exposure, as shown by Luminex xMAP quantification), and repeated aliquotization to new tubes may cause profoundly lower measures of Aβs (Tsukie and Kuwano, unpublished data, 2010). This may partly explain why absolute levels of Aβs in CSF greatly vary among laboratories, whereas their relative ratios (*e.g.* Aβ42/40) seem to be roughly consistent. The CSF concentrations of Aβ38, 40 and 42 were quantified using commercially available ELISA kits (Cat no. 27717, 27718 and 27712, respectively, IBL, Gunma, Japan). To measure Aβ43, anti-Aβ43 polyclonal antibody as a capture antibody was combined with amino terminus-specific antibody (82E1) (Cat no. 10323, IBL, Gunma, Japan) as a detector antibody. The detection limit of Aβ43 quantified by the ELISA was 0.78 pM (data not shown). Thus all ELISAs used here detect Aβ1-x, but not amino-terminally truncated Aβs. The specificities of ELISAs are provided in Supporting Information Fig S1.

CSF immunoprecipitation and Western blotting

When required, CSF Aβs were immunoprecipitated with protein G-sepharose conjugated with 82E1 at 4°C by keeping a container in gentle rotation overnight. The mixture was centrifuged at 10,000×g for 5 min, and resultant pellets were then washed twice with phosphate-buffered saline. The washed beads were suspended with the Laemmli sample buffer for SDS–polyacrylamide gel electrophoresis (SDS–PAGE). The immunoprecipitated Aβs were separated on Tris/Tricine/8 M urea gels (Kakuda et al, 2006), followed by Western blotting using 82E1. To immunodetect Aβ42 and Aβ43, Aβ42 monoclonal antibody (44A3, IBL) and Aβ43 polyclonal antibody (IBL) were used (Supporting Information Fig S3).

Numerical simulation based on the stepwise processing model of γ-secretase

The temporal profiles for the ratios of Aβ40/43 and Aβ38/42 were simulated based on the stepwise processing model. Parameters including rate constants were set to fit maximally the temporal profile of the cleaving activity in the reconstituted γ-secretase system (Takami et al, 2009).

We set the condition that βCTF substrate is supplied steadily from the external source. When βCTF supply is balanced roughly in the order with γ-secretase processing rate, the stepwise-processing model was found to have the two successive steady states, with each accompanying linear changes in [ES] or [S] concentrations. The first steady state is just after the initial transition period that corresponds to the acute saturation phase of γ-secretase with βCTF. The second steady state is associated with the constant concentrations of the enzyme/substrate complex except ES38 and ES40. Because these steady states kept the ratios of Aβ38/Aβ40 and Aβ42/Aβ43 constant, the simulation was quite consistent with the CSF data.

Quantification of human brain raft-associated γ-secretase activity

Since γ-secretase is thought to be concentrated in rafts (Hur et al, 2008; Wada et al, 2003), we measured raft-associated γ-secretase activity rather than CHAPSO-solubilized activity. Rafts were prepared from human brains which were frozen within 12 h postmortem, as previously described (Oshima et al, 2001; Wada et al, 2003) with some modifications. We do not know exactly whether the γ-secretase activity depends upon the sampling site. In our hands, there appear no large differences in the activity among the sampled sites in a given prefrontal slice. No significant differences in the activity were noted between outer and inner layer of the cortex. After carefully removing leptomeninges and blood vessels, small (<0.5 g) blocks from prefrontal cortices (Brodmann areas 9–11) were homogenized in ~10 volumes of 10% sucrose in MES-buffered saline (25 mM MES, pH 6.5, and 150 mM NaCl) containing 1% CHAPSO and various protease inhibitors. The homogenate was adjusted to 40% sucrose by the addition of an equal volume of 70% sucrose in MES-buffered saline, placed at the bottom of an ultracentrifuge tube, and overlaid with 4 ml of 35% sucrose and finally with 4 ml of 5% sucrose in MES-buffered saline. The discontinuous gradient was centrifuged at 39,000 rpm for 20 h at 4°C on a SW 41 Ti rotor (Beckman, Palo

The paper explained

PROBLEM:

Alzheimer's disease is a devastating form of progressive dementia, in which senile plaques composed of Aβ form in the brain. Different species of Aβ are derived from APP through sequential cleavage by β- and γ-secretases and can be detected in the CSF of patients. These can serve as markers for the disease.

RESULTS:

We investigated why CSF concentrations of Aβ42 are lower in MCI and AD patients. We suggest that this is not because Aβ42/43 is selectively deposited in the brain, but because γ-secretase activity is altered in AD brain: more Aβ42 and Aβ43 are converted to Aβ40 and Aβ38, respectively, resulting in lower Aβ42 and Aβ43 in CSF.

IMPACT:

Our results predict that γ-secretase modulators would have only limited efficacy in treatment of AD patients, because Aβ42/43 production by γ-secretase is already shifted towards reduced levels in AD brain.

Alto, CA). An interface of 5%/35% sucrose (fraction 2) was carefully collected (referred to as raft fraction). Raft fractions were recentrifuged after dilution with buffer C (20 mM PIPES, pH 7.0, 250 mM sucrose and 1 mM EGTA). The resultant pellet was washed twice and resuspended with buffer C, which was kept at −80°C until use.

As the method of measuring the raft γ-secretase activity was not yet established, we first determined the assay conditions. The incubation of raft fraction with βCTF generated exactly the same tri- and tetrapeptides we previously observed in the detergent-soluble γ-secretase assay system (Takami et al, unpublished observation). This suggests that the cleavage by raft-associated γ-secretase proceeds in the identical manner as by CHAPSO-reconstituted γ-secretase (Takami et al, 2009). In our hands, preexisting βCTF bound in rafts generated only negligible amounts of Aβs, and their generation was dependent exclusively on exogenously added βCTF. Thus, we concluded that the addition of βCTF to raft fraction make possible to measure the raft-associated γ-secretase activity, although we do not know how the exogenously added βCTF is integrated into raft, gets access to and is degraded by raft-embedded γ-secretase. Using this assay method, the activities of raft-associated γ-secretase in human brains were found to be only a little affected postmortem, when compared with that prepared from fresh rat brains. A progressive decline in the activity was barely detectable from 4 to 17 h postmortem. The discrepancy in the postmortem decay between our and the previous data (Hur et al, 2008) would be ascribed to the assay method: the latter are based on the activity measured by using endogenous (raft-bound) substrate that is also susceptible to proteolytic degradation (Hur et al, 2008).

Each raft fraction, adjusted to 100 μg/ml in protein concentration, was incubated with 200 nM C99FLAG for 2 h at 37°C (Kakuda et al, 2006). The produced Aβs were separated on SDS–PAGE, and subjected to quantitative Western blotting, using specific antibodies, 3B1 for Aβ38, BA27 for Aβ40, 44A3 for Aβ42 and anti-Aβ43 polyclonal for Aβ43.

Statistical analysis

All statistical analyses were performed using SPSS version 14.0. The results were expressed as means ± standard deviations. Because data transformations were required to achieve normally distributed data, all analyses including Aβ38, Aβ40, Aβ42 and Aβ43 were performed after a logarithmic transformation. Pearson's correlation coefficients were calculated to indicate the strength of the linear relationship between two variables. An ANOVA was used to test the equality of mean values of continuous variables among three groups, that is control, MCI and AD. Multiple comparisons were done by Dunnett's *t*-test, Bonferroni's *t*-test and Welch's *t*-test between control and MCI/AD, and among three groups, respectively. A two-tailed *p*-value of <0.05 was considered to be statistically significant.

Author contributions

NK, MT, KN, YI: measurement of raft-associated γ-secretase activity in human brains, LC-MS/MS confirmation of released peptides, ELISA quantification of Aβ38, 40, 42 and 43 in CSF and tissue blocks, and experimental design of the present work; MS, HiA, KF, TI, and the Japanese Alzheimer's Disease Neuroimaging Initiative: collection of CSF samples from controls, MCI/AD patients; YH, MM, HaA: collection of CSF from iNPH patients; HY, SM, HH: Aβ immunocytochemistry of tissue sections from brains with various SP stages (Braak); KA: statistical analysis; RK: establishment of the appropriate Aβ quantification conditions; YN: simulation of the stepwise processing model.

Acknowledgements

We thank Dr. Haruhiko Akiyama, Department of Psychogeriatrics, Tokyo Institute of Psychiatry, Tokyo Metropolitan Organization for Medical Research, Tokyo, for the help in the initial phase of this study, and Dr. Takaomi C. Saido, RIKEN Brain Science Institute, for sharing the data on his R278I transgenic mice. Dr. Makoto Higuchi, Molecular Imaging Center, National Institute of Radiological Sciences, Chiba, kindly provided us with aged Tg2576 littermates. This project was supported by New Energy and Industrial Technology Development Organization in Japan (J-ADNI).

Supporting Information is available at EMBO Molecular Medicine online.

The authors declare that they have no conflict of interest.

References

Adachi T, Saito Y, Hatsuta H, Funabe S, Tokumaru AM, Ishii K, Arai T, Sawabe M, Kanemaru K, Miyashita A, *et al* (2010) Neuropathological asymmetry in argyrophilic grain disease. J Neuropathol Exp Neurol 69: 737-744

Hong S, Quintero-Monzon O, Ostaszewski BL, Podlisny DR, Cavanaugh WT, Yang T, Holtzman DM, Cirrito JR, Selkoe DJ (2011) Dynamic analysis of amyloid β-protein in behaving mice reveals opposing changes in ISF versus parenchymal Aβ during age-related plaque formation. J Neurosci 31: 15861-15869

Hur JY, Welander H, Behbahani H, Aoki M, Frånberg J, Winblad B, Frykman S, Tjernberg LO (2008) Active gamma-secretase is localized to detergent-resistant membranes in human brain. FEBS J 275: 1174-1187

Ishikawa M, Hashimoto M, Kuwana N, Mori E, Miyake H, Wachi A, Takeuchi T, Kazui H, Koyama H (2008) Guidelines for management of idiopathic normal pressure hydrocephalus. Neurol Med Chir (Tokyo) 48: S1-S23

Iwatsubo T, Odaka A, Suzuki N, Mizusawa H, Nukina N, Ihara Y (1994) Visualization of Aβ42(43) and Aβ40 in senile plaque with end-specific Aβ monoclonals: evidence that an initially deposited forms is Aβ42(43). Neuron 13: 45-53

Kakuda N, Funamoto S, Yagishita S, Takami M, Osawa S, Dohmae N, Ihara Y (2006) Equimolar production of amyloid β-protein and amyloid precursor protein intracellular domain from β-carboxyl-terminal fragment by γ-secretase. J Biol Chem 281: 14776-14786

Kawarabayashi T, Younkin LH, Saido TC, Shoji M, Ashe KH, Younkin SG (2001) Age-dependent changes in brain, CSF, and plasma amyloid (β) protein in the Tg2576 transgenic mouse model of Alzheimer's disease. J Neurosci 21: 372-381

Kosaka T, Imagawa M, Seki K, Arai H, Sasaki H, Tsuji S, Asami-Odaka A, Fukushima T, Imai K, Iwatsubo T (1997) The βAPP717 Alzheimer mutation increases the percentage of plasma amyloid-beta protein ending at Aβ42(43). Neurology 48: 741-745

Kuwano R, Miyashita A, Arai H, Asada T, Imagawa M, Shoji M, Higuchi S, Urakami K, Kakita A, Takahashi H, *et al* (2006) Dynamin-binding protein gene on chromosome 10q is associated with late-onset Alzheimer's disease. Hum Mol Genet 15: 2170-2182

Li G, Aryan M, Silverman JM, Haroutunian V, Perl DP, Birstein S, Lantz M, Marin DB, Mohs RC, Davis KL (1997) The validity of the family history method for identifying Alzheimer disease. Arch Neurol 54: 634-640

McKhann G, Drachman D, Folstein M, Katzman R, Price D, Stadlan EM (1984) Clinical diagnosis of Alzheimer's disease: report of the NINCDS-ADRDA Work Group under the auspices of Department of Health and Human Services Task Force on Alzheimer's Disease. Neurology 34: 939-944

Nakaya Y, Yamane T, Shiraishi H, Wang HQ, Matsubara E, Sato T, Dolios G, Wang R, De Strooper B, Shoji M, *et al* (2005) Random mutagenesis of presenilin-1 identifies novel mutants exclusively generating long amyloid β-peptides. J Biol Chem 280: 19070-19077

Oshima N, Morishima-Kawashima M, Yamaguchi H, Yoshimura M, Sugihara S, Khan K, Games D, Schenk D, Ihara Y (2001) Accumulation of amyloid beta-protein in the low-density membrane domain accurately reflects the extent of beta-amyloid deposition in the brain. Am J Pathol 158: 2209-2218

Qi-Takahara Y, Morishima-Kawashima M, Tanimura Y, Dolios G, Hirotani N, Horikoshi Y, Kametani F, Maeda M, Saiso TC, Wang R, *et al* (2005) Longer forms of amyloid β protein: implications for the mechanism of intramembrane cleavage by γ-secretase. J Neurosci 25: 436-445

Ringman JM, Younkin SG, Pratico D, Seltzer W, Cole GM, Geschwind DH, Rodriguez-Agudelo Y, Schaffer B, Fein J, Sokolow S, *et al* (2008) Biochemical markers in persons with preclinical familial Alzheimer disease. Neurology 71: 85-92

Saito T, Suemoto T, Brouwers N, Sleegers K, Funamoto S, Mihira N, Matsuba Y, Yamada K, Nilsson P, Takano J, *et al* (2011) Potent amyloidogenicity and pathogenicity of Aβ43. Nat Neurosci 14: 1023-1032

Scheuner D, Eckman C, Jensen M, Song X, Citron M, Suzuki N, Bird TD, Hardy J, Hutton M, Kukull W, *et al* (1996) Secreted amyloid β-protein similar to that in the senile plaques of Alzheimer's disease in increase in vivo by the presenilin 1 and 2 and APP mutations linked to familial Alzheimer's disease. Nat Med 2: 864-870

Schoonenboom NS, Mulder C, Van Kamp GJ, Mehta SP, Scheltens P, Blankenstein MA, Mehta PD (2005) Amyloid β 38, 40, and 42 species in cerebrospinal fluid: more of the same. Ann Neurol 58: 139-142

Selkoe DJ (2001) Alzheimer's disease: genes, proteins, and therapy. Physiol Rev 81: 741-766

Serneels L, Van Biervliet J, Craessaerts K, Dejaegere T, Horre K, Van Houtvin T, Esselmann H, Paul S, Schafer MK, Berezovska O, *et al* (2009) γ-Secretase heterogeneity in the Aph1 subunit: relevance for Alzheimer's disease. Science 324: 639-642

Shoji M, Matsubara E, Kanai M, Watanabe M, Nakamura T, Tomidokoro Y, Shizuka M, Wakabayashi K, Igeta Y, Ikeda Y, *et al* (1998) Combination assay of CSF tau, Aβ1–40 and Aβ 1–42(43) as a biochemical marker of Alzheimer's disease. J Neurol Sci 158: 134-140

Silverberg GD, Mayo M, Saul T, Rubenstein E, McGuire D (2003) Alzheimer's disease, normal-pressure hydrocephalus, and senescent changes in CSF circulatory physiology: a hypothesis. Lancet Neurol 2: 506-511

Simonsen AH, Hansson SF, Ruetschi U, McGuire J, Podust VN, Davies HA, Mehta P, Waldemar G, Zetterberg H, Andreasen N, *et al* (2007) Amyloid β1–40 quantification in CSF: comparison between chromatographic and immunochemical methods. Dement Geriatr Cogn Disord 23: 246-250

Takami M, Nagashima Y, Sano Y, Ishihara S, Morishima-Kawashima M, Funamoto S, Ihara Y (2009) γ-Secretase: successive tripeptide and tetrapeptide release from the transmembrane domain of β-carboxyl terminal fragment. J Neurosci 29: 13042-13052

Takasugi N, Tomita T, Hayashi I, Tsuruoka M, Niimura M, Takahashi Y, Thinakaran G, Iwatsubo T (2003) The role of presenilin cofactors in the γ-secretase complex. Nature 422: 438-441

Wada S, Morishima-Kawashima M, Qi Y, Misonou H, Shimada Y, Ohno-Iwashita Y, Ihara Y (2003) Gamma-secretase activity is present in rafts but is not cholesterol-dependent. Biochemistry 47: 13977-13986

Weggen S, Eriksen JL, Das P, Sagi SA, Wang R, Pietrzik CU, Findlay KA, Smith TE, Murphy MP, Bulter T, *et al* (2001) A subset of NSAIDs lower amyloidogenic Aβ42 independently of cyclooxygenase activity. Nature 414: 212-216

Winblad B, Palmer K, Kivipelto M, Jelic V, Fratiglioni L, Wahlund LO, Nordberg A, Backman L, Albert M, Almkvist O, *et al* (2004) Mild cognitive impairment—beyond controversies, towards a consensus: report of the International Working Group on Mild Cognitive Impairment. J Intern Med 256: 240-246

Yang DS, Tandon A, Chen F, Yu G, Yu H, Arakawa S, Hasegawa H, Duthie M, Schmidt SD, Ramabhadran TV, *et al* (2002) Mature glycosylation and trafficking of nicastrin modulate its binding to presenilins. J Biol Chem 277: 28135-28142

Zou K, Yamaguchi H, Akatsu H, Sakamoto T, Ko M, Mizoguchi K, Gong JS, Yu W, Yamamoto T, Kosaka K, *et al* (2007) Angiotensin-converting enzyme converts amyloid β-protein 1–42 (Aβ(1–42)) to Aβ(1–40), and its inhibition enhances brain Aβ deposition. J Neurosci 27: 8628-8635

Journal of Neuroscience Research

Journal of Neuroscience Research 89:815–821 (2011)

Dissociation of β-Amyloid From Lipoprotein in Cerebrospinal Fluid From Alzheimer's Disease Accelerates β-Amyloid-42 Assembly

Ayumi Takamura,[1,2] Takeshi Kawarabayashi,[2] Tatsuki Yokoseki,[3] Masao Shibata,[3] Maho Morishima-Kawashima,[4] Yuko Saito,[5] Shigeo Murayama,[5] Yasuo Ihara,[6] Koji Abe,[7] Mikio Shoji,[2] Makoto Michikawa,[1] and Etsuro Matsubara[1,2]*

[1]Department of Alzheimer's Disease Research, Research Institute, National Center for Geriatrics and Gerontology, Aichi, Japan
[2]Department of Neurology, Institute of Brain Science, Hirosaki University Graduate School of Medicine, Aomori, Japan
[3]Immunas Pharma Inc., Kanagawa, Japan
[4]Department of Molecular Neuropathology, Faculty of Pharmaceutical Sciences, Hokkaido University, Hokkaido, Japan
[5]Department of Neuropathology, Tokyo Metropolitan Institute of Gerontology, Tokyo, Japan
[6]Department of Neuropathology, Faculty of Life and Medical Sciences, Doshisha University, Kyoto, Japan
[7]Department of Neurology, Okayama University School of Medicine, Okayama, Japan

Monoclonal 2C3 specific to β-amyloid (Aβ) oligomers (AβOs) enabled us to test our hypothesis that the alteration of lipoprotein–Aβ interaction in the central nervous system (CNS) initiates and/or accelerates the cascade favoring Aβ assembly. Immunoprecipitation of frontal cortex employing 2C3 unequivocally detected soluble 4-, 8-, and 12-mers in Alzheimer's disease (AD) brains. Immunoblot analysis of the entorhinal cortex employing 2C3 revealed that the accumulation of soluble 12-mers precedes the appearance of neuronal loss or cognitive impairment and is enhanced as the Braak neurofibrially tangle (NFT) stages progress. The dissociation of soluble Aβ from lipoprotein particles occurs in cerebrospinal fluid (CSF), and the presence of lipoprotein-free oligomeric 2C3 conformers (4- to 35-mers) was evident, which mimic CNS environments. Such CNS environments may strongly affect conformation of soluble Aβ peptides, resulting in the conversion of soluble $A\beta_{42}$ monomers into soluble $A\beta_{42}$ assembly. The findings suggest that functionally declined lipoproteins may accelerate the generation of metabolic conditions leading to higher levels of soluble $A\beta_{42}$ assembly in the CNS.

Key words: Alzheimer's disease; Aβ; lipoprotein; oligomer; monomer

Accumulating lines of evidence indicate that memory loss represents a synaptic failure caused directly by soluble β-amyloid (Aβ) oligomers (AβOs; Klein et al., 2001; Selkoe, 2002; Hass and Selkoe, 2007). The possible mechanism underlying the neurotoxic action of AβOs has been postulated as neurotoxic ligands (Lambert et al., 1998; Walsh et al., 2002; Chromy et al., 2003; Gong et al., 2003; Lacor et al., 2004; Cleary et al., 2005; Lesné et al., 2006; Shankar et al., 2008; Noguchi et al., 2009), iron channel formation (Lin et al., 2001; Quist et al., 2005), pore formation (Lashuel et al., 2002; Kayed et al., 2009), and dysfunction of cholesterol metabolism in neurons (Michikawa et al., 2001; Gong et al., 2002; Zou et al., 2002). However, the exact metabolic conditions controlling the in vivo generation of soluble AβOs remain unknown. It is well known that aging is the most prevailing risk factor for sporadic AD. In vivo studies have shown that Aβ neurotoxicity is closely related to the brain aging via unknown age-related factors (Geula et al., 1998), perhaps reflecting metabolic alterations. Notably, the APOE genotype is also the major genetic risk factor for late-onset sporadic AD (Schmechel et al., 1993; Tanzi and Bertram, 2001; Wellington, 2004). HDL-like lipoproteins, mainly

Contract grant sponsor: Ministry of Education, Culture, Sports, Science and Technology, Japan (to E.M.); Contract grant sponsor: the Program for Promotion of Fundamental Studies in Health Sciences of the National Institute of Biomedical Innovation (NIBIO; to E.M.).

*Correspondence to: Etsuro Matsubara, Department of Neurology, Institute of Brain Science, Hirosaki University Graduate School of Medicine, 5 Zaifu, Hirosaki, Aomori 036-8216, Japan. E-mail: etsuro@cc.hirosaki-u.ac.jp

Received 7 September 2010; Revised 17 December 2010; Accepted 11 January 2011

Published online 10 March 2011 in Wiley Online Library (wileyonlinelibrary.com). DOI: 10.1002/jnr.22615

lipidated apoE, are in charge of cholesterol transport to and from neurons (Michikawa et al., 2001; Gong et al., 2002), in which cholesterol metabolism is quite different from that in systemic circulation. In addition to lipid trafficking, apoE as a form of HDL-like lipoprotein plays a major role in Aβ metabolism in the central nervous system (CNS). Under physiological conditions, HDL-like lipoproteins unequivocally interact with soluble Aβ in cerebrospinal fluid (CSF; Koudinov et al., 1996). Interestingly, when the generation of HDL-like lipoproteins in the AD mouse model is suppressed or overexpressed via the specific regulation of ATP-binding cassette A1 (ABCA1), Aβ deposition exhibits augmentation or reduction, respectively, which depends on the degree of ABCA1-mediated lipidation of apoE in the CNS (Wahrle et al., 2005, 2008). From these points of view, lipidic environments in the CNS represent one of the prevailing metabolic conditions. We hypothesized that an alteration of the lipoprotein–sAβ interaction in the CNS is capable of initiating and/or accelerating the cascade favoring Aβ assembly. Actually, we demonstrate that functionally declined lipoproteins may be the major determinants in the generation of metabolic conditions leading to higher levels of the soluble dimeric form of Aβ in AD brains (Matsubara et al., 1999, 2004). To verify this hypothesis and extend previous observations (Matsubara et al., 1999, 2004), we focused on the entorrhinal cortex (EC) as well as CSF, which mimics CNS environments, followed by biochemical analyses using an antioligomer specific antibody. The presence of lipoprotein-free soluble AβOs in CSF was assessed in age-matched normal controls (NCs) and patients with Alzheimer's disease (AD) by size-exclusion chromatography (SEC) and enzyme-linked immunosorbent assay (ELISA) specific for either AβOs or AβMs to test our hypothsis.

MATERIALS AND METHODS

Generation of Monoclonal 2C3

Monoclonal 2C3, which is specific to AβOs with a molecular mass larger than tetramers (unpublished data), was generated and characterized as described elsewhere.

Patients

CSF samples (5 ml) were collected from 13 age-matched normal controls (NCs; 70.6 ± 8.2 years old) and 12 AD patients (73.2 ± 7.8 years old) after 12 hr of fasting. None of the individuals in the two groups had a history of stroke or other neurological conditions in the CNS that might have affected their lipoprotein profile, and none was taking drugs known to affect lipid metabolism. The diagnosis of AD was made in accordance with the NINCDS-ADRDA criteria, and only those who met the criteria of probable AD were included.

Lipoprotein Separation and Depletion

After separation of CSF collected from 12 patients with AD and 13 NCs, lipoprotein depletion was carried out by preparative sequential density flotation ultracentrifugation using 600 μl of CSF and a protocol previously described (Matsubara et al., 2004). Briefly, the density of the collected CSF was adjusted to 1.25 g/ml using KBr, and the CSF was ultracentrifuged at 100,000 rpm for 8 hr at 16°C using a Hitachi RP100AT rotor. The infranatant at a density of 1.25 g/ml, named lipoprotein-depleted CSF (LPD-CSF), and the floated lipoproteins were subjected to ultrafiltration using a 3-kDa cutoff membrane (Microcon 3; Amicon, Inc.) and stored either frozen or at 4°C until use.

SEC

SEC (molecular exclusion, 2×10^6; void volume varied from fraction (Fr.) 7 to Fr. 9 enabled us to separate specifically not only AβMs from AβOs, but also lipoprotein-associated Aβ from lipoprotein-free Aβ, as previously reported (Matsubara et al., 2004). The Aβ species either in whole CSF or in lipoprotein-depleted CSF were fractionated on a Superose 12 size-exclusion column (1 cm × 30 cm; Pharmacia, Uppsala, Sweden) equilibrated with the corresponding mobile-phase solution at a flow rate of 0.5 ml/min. Twenty-eight fractions of 1 ml each were collected and analyzed. Lipoprotein was depleted as described previously (Matsubara et al., 2004). Details are also described below. To determine where Aβ eluted, a 100-μl aliquot from each fraction was analyzed in a BNT77-BC05 or BNT77-BA27 enzyme-linked immunosorbent assay (ELISA) as described previously in detail (Matsubara et al., 2004). For evaluation of lipids, total cholesterol levels were enzymatically measured using a standard kit (Wako, Osaka, Japan). Under our experimental conditions, CSF lipoproteins were eluted in Frs. 7–14, whereas Frs. 15–28 contained cholesterol-free proteins. To determine further where the Aβ oligomers eluted, a 100-μl aliquot from each fraction was analyzed by 2C3-based oligomer sandwich ELISA.

Human Tissue Subjects and Extractions

The current study is based on autopsy cases (n = 50; 26 men, 24 women) from the Brain Bank at the Tokyo Metropolitan Institute of Gerontology (Itabashi, Tokyo, Japan). All of the subjects and the sampling methods were reported previously in detail (Katsuno et al., 2005). In this project, we focused on the soluble brain fraction, which was not characterized in a previous study (Katsuno et al., 2005). Briefly, frozen tissue samples (the anterior portion of the entorhinal cortex) were homogenized in 9 volumes of Tris-saline (TS) buffer containing a cocktail of protease inhibitors as described previously (Katsuno et al., 2005). The homogenates were centrifuged at 265,000*g* for 20 min. One-third (0.5 ml) of the homogenates was subjected to 2C3 immunoblot analysis.

ELISA Specific for Either AβMs or AβOs in CSF

After informed consent had been obtained, CSF samples were collected and stored in the human resource bank of the Department of Neurology, Okayama University School of Medicine. All human age-matched CSF samples were randomly selected from this bank and used for this study. To characterize the presence of AβOs in CSF, the CSF samples were subjected to SEC as described above. To determine